Strain Rate Characterization of Paperboard Materials used in Packaging Materials

Zichun Wang

2022

LUND UNIVERSITY

LTH

FACULTY OF ENGINEERING

MASTER THESIS
DIVISION OF PRODUCTION AND MATERIALS ENGINEERING
LUND UNIVERSITY

ISBN: LUTMDN/(TMMV-5345)/1-56/2022
Supervisor: Dmytro Orlov, Professor
Industrial Supervisor: Eskil Andreasson, Dr., Tetra Pak®
Examiner: Jinming Zhou, Professor

Author: Zichun Wang
Lund, Sweden 2022

Avdelningen för Industriell Produktion
Lunds Tekniska Högskola
Lunds universitet
Box 118
221 00 Lund
Sverige

Division of Production and Materials Engineering
LTH, School of Engineering
Lund University
Box 118
SE-221 00 Lund
Sweden

Printed in Sweden
Media-Tryck
Lund University

Foreword

First of all I would like to thank my main supervisor at LTH, Prof. Dmytro Orlov, without his help, advice and expertise it would have been difficult to start my research. Secondly, I would like to thank my co-supervisor Dr. Eskil Andreasson from Tetra Pak® for his answers to many practical questions, especially for the time he spent searching for articles related to this thesis and for taking me on a tour and understanding of the actual production plant at Tetra Pak® in Lund. I am very grateful to my examiner, Prof. Jinming Zhou, for reading and checking the report. I would also like to thank all the people in the department and Tetra Pak® who helped me by discussing various issues with me and helping me to prepare my lab samples.

Lund 2022-05-22

Zichun Wang

Sammanfattning

I detta examensarbete introducerades först den grundläggande kunskapen om förpackningsmaterial genom en litteraturstudie med fokus på att utforska effekten av belastningshastighet på mekaniska egenskaper hos kartongmaterial. Med hjälp av dragprov och mikroskopiska observationer analyserades förändringarna av mekaniska egenskaper som t.ex. sträckgräns, töjning och Youngs modul hos de två olika kartonger som används i laminerade förpackningsmaterial för de två olika förpackningstyperna Tetra Fino® Aspetic och Tetra Brik® Aseptic från Tetra Pak® vid en töjningshastighet som varierade från 0,0167 s^{-1} till 1,67 s^{-1}. Kartongprovernas elasticitet ökade först och minskade sedan i detta intervall, och det högsta värdet erhölls vid cirka 0,167 s^{-1}. Töjningen var i princip positivt korrelerad med töjningshastigheten, och young-modulen var inte signifikant relaterad till den.

Nyckelord: Kartong, töjningshastighet, flytspänning.

Abstract

This master thesis firstly introduced the basic knowledge of packaging materials through a literature survey focused on exploring the effect of strain-rate on mechanical properties of paperboard materials. By means of tensile tests and microscopic observation, the changes of mechanical properties such as yield strength, strain and Young's modulus of the two different paperboards used in laminated packaging materials for the two different package types Tetra Fino® Aspetic (TFA) and Tetra Brik® Aseptic (TBA) from Tetra Pak® were analyzed at strain rate ranging from 0.0167 s^{-1} to 1.67 s^{-1}. The yield strengths of the paperboard samples were first increased and then decreased in this strain-rate range, and the maximum value was obtained at about 0.167 s^{-1}. The strain was basically positively correlated with the strain rate, and the Young's modulus was not significantly related to it.

Keywords: Paperboard, Strain rate, yield stress.

List of Abbreviations

Full name	Abbreviation
chemical-thermal-mechanical pulps	CTMP
cross-machine direction	CD
Lunds Tekniska Högskola	LTH
machine direction	MD
out-of-plane direction	ZD
polyethylene	PE
Scanning Electron Microscope	SEM
Tetra Brik® Aseptic	TBA
Tetra Fino® Aseptic	TFA

Table of Content

1. Introduction

Tetra Pak®, established in Lund Sweden, by Dr. Ruben Rausing in 1951, is one of the leading companies globally in food packaging solutions, especially for liquid food. Working closely with customers and suppliers, they provide safe, innovative and environmentally sound products. This thesis is conducted in collaboration with Tetra Pak® Packaging Solutions AB in Lund and is devoted to the study of mechanical properties, especially the effect of strain rate on paperboard materials used in the packaging materials.

In the packaging materials, mechanical properties are very important in both fabrication of package and service. Mechanical properties of packaging materials include stiffness, tensile strength, impact resistance, tear strength and so on. Materials with good performance in the above properties, such as paperboard, aluminum foil and polymer, become suitable packaging materials and have a wide range of applications. Typical example of packaging material produced by Tetra Pak is presented in Figure 1.1. Paperboard provides the primary stiffness and strength for the material system, while aluminum foil prevents light and oxygen from getting in, and natural or artificial polymer layers act as moisture-proof layers and adhesives.

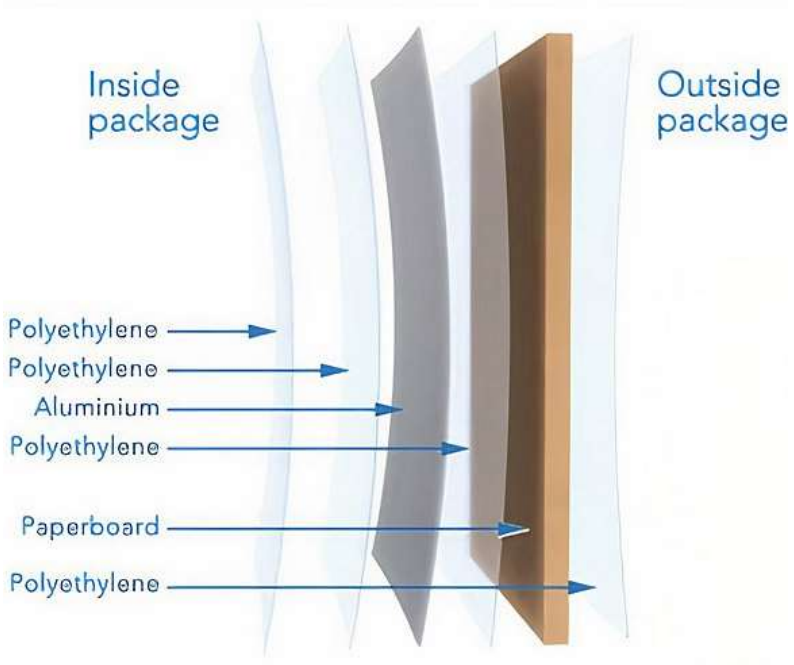

Figure 1.1: *Packaging material layers for a typical Tetra Pak® carton package* [1]

Modern technology for packaging food in filling machines takes place at very high rates, which has a maximum speed of 40 000 packages/hour in the hyper speed filling machines today [17]. With the increase of strain rate, mechanical properties such as yield strength, ultimate tensile strength and elongation change. As a consequence, the study of mechanical behavior of packaging materials at high strain rate is critically important. Preliminary literature survey on strain-rate material responses reveals very limited number of existing studies on this topic that cover strain rates well below those in food packaging using machines designed by Tetra Pak.

Therefore, this project has been initiated by Tetra Pak® for carrying out in-depth literature survey in the core and closely relevant areas and experimental investigation of the effect of strain rate on tensile behavior of different packaging materials. It is expected to play an important role in the development of packaging materials technology at Tetra Pak.

The main objectives of this project are to:

1) Carry out a comprehensive literature survey on state-of-the-art in packaging materials and the effect of strain rate on their mechanical properties.
2) Study experimentally the effect of strain rate on the mechanical properties and fracture of two most common paperboards used in packaging materials at Tetra Pak.
3) Make recommendations for optimizing manufacturing process at Tetra Pak taking into consideration the results of present work.

2. Paperboard in packaging materials

The purpose of this section is to analyze state-of-the-art knowledge of

- Packaging materials for liquid food.
- Mechanical properties of packaging materials including anisotropy.
- Effect of strain rate on the mechanical properties of packaging materials.
- Experimental methods for determining the mechanical properties of packaging materials at high strain rates.
- Mathematical models describing the stress-strain behavior of packaging materials.

Therefore, this study requires reviewing latest information available in public sources, followed by mechanical testing experiments and microscopic and macroscopic analyses.

2.1. Packaging materials

The packaging materials developed by Tetra Pak® consist of paperboard, polyethylene and aluminum foil to protect against outside moisture, oxygen and light, which is benefit for maintaining the nutritional value and flavors of the food in the package in ambient temperatures.**Error! Reference source not found.** Schematic illustration of a material typically used for packaging beverages is presented in Figure 2.1.

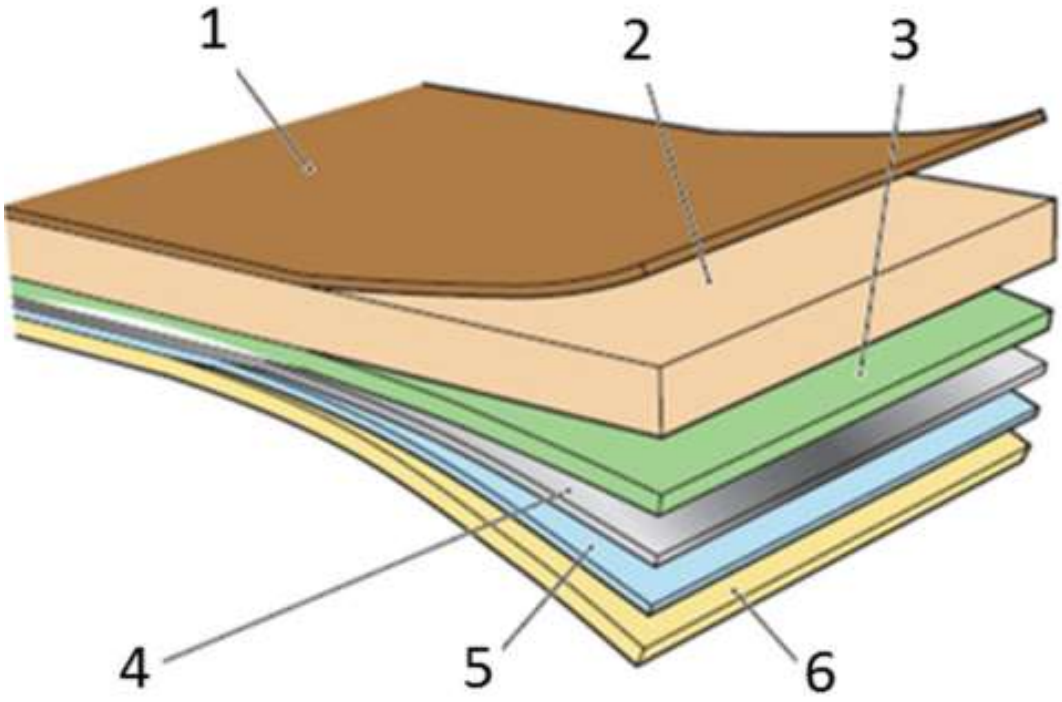

Figure 2.1: *Typical composition and functionality of beverage packaging material*[4]

The following are the specific functions of the different layers:

(1) external plastic layer, protects against outside moisture and enables sealing;

(2) paperboard, gives stability and strength and enables printing;

(3) lamination layer, enables adhesion between aluminum foil and paperboard;

(4) aluminum foil, acts as oxygen, flavor and light barrier;

(5) adhesion layer between the aluminum foil and the internal plastic layer;

(6) internal plastic layer, seals in the liquid product and enables hermetical closure.[4]

The outermost layer (1) is usually polyethylene (PE) making the package waterproof and its contents antibacterial. The following paperboard layer (2) is mainly used to increase the strength of the packaging material. Therefore, its mechanical properties are important, and thus also become the focus of research in this project's. The lamination layer (3) is also made of PE. The aluminum foil layer (4) plays an important role in preserving the freshness of food. The material of the (5) layer is low-density polyethylene (LDPE) which acts as a binding layer. The internal layer (6) material is PE to seal off the liquid contents. As can be seen from the types of materials and the role of the different layers, the study of the mechanical properties of paperboard is of great significance for the optimization of Tetra Pak's packaging materials.

2.2. Role of paperboard in packaging materials

Paperboard-based composites are an ideal material for packaging applications including food and beverage packaging. This is because paperboard is a lightweight cellulose fiber material with a high degree of anisotropy between in-plane and out-of-plane properties, and its high bending stiffness makes it an excellent material for packaging containers. The carton itself is made of wood fiber, and its natural properties make experimental evaluation and material modelling of paperboard and its driving laminate composites challenging.[2]

There are three main sub-layers of food packaging paperboard: the top, middle and bottom layers. In order to produce paperboard with high bending stiffness and light weight, the outer layer is usually made of chemical pulp, whose mechanical and physical properties are characterized by high hardness and density. The mid layers are made from a combination of mechanical, chemical, or chemical-thermal-mechanical pulps (CTMP) to reduce thickness and are more suitable for obtaining a well-defined shape and layering profile during conversion. For the food packaging applications paperboards with a thickness of almost 350-500 μm are applied and the stiffer outer layers have thickness of 80-120 μm.[3]

Chemical processes typically produce higher pulp strength and paper quality, and more efficient reuse of chemicals and energy than mechanical processes. CTMP is a semi-mechanical pulping method, which is a combination of chemical and mechanical pulping. The process uses heat to degrade the lignin, giving a lower yield of pulp, but better quality than mechanical pulping. The paperboard material manufactured by the above two methods can meet the basic needs of the second layer in the packaging. Figure 2.2 shows the schematic diagram of CTMP.[18]

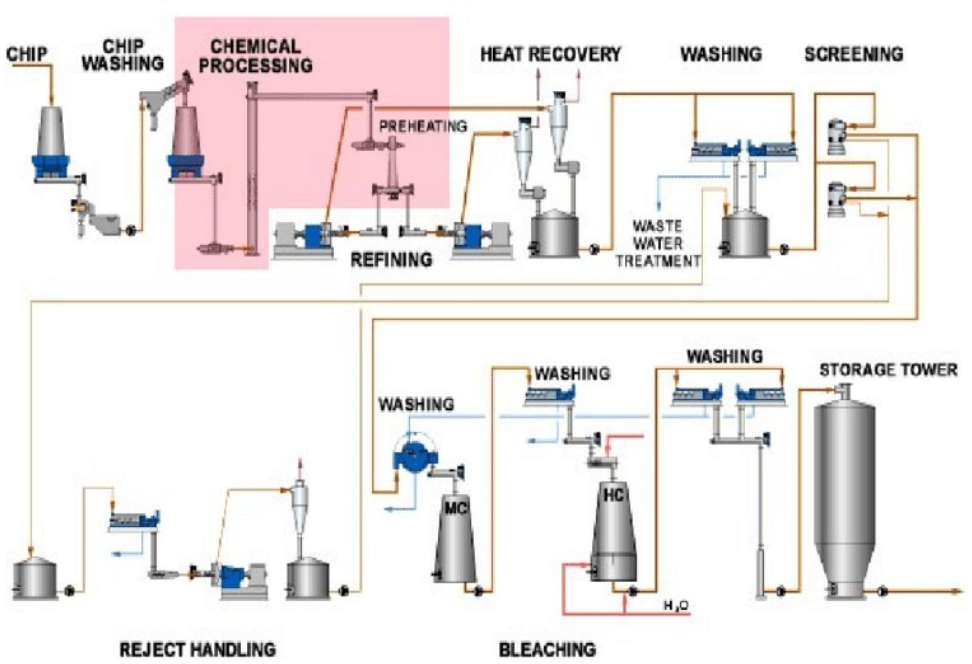

Figure 2.2: *CTMP process in paperboard production[18]*

2.2.1. Microstructure of paperboard

It is well known that the properties of a material are closely related to its microstructure, such as the size and arrangement of crystals in inorganic materials, and the fiber orientation of the paperboard material in this project. Therefore, it is necessary to conduct microscopic image studies.

The following Figure 2.3 and Figure 2.4 show Scanning Electron Microscope (SEM) images of the two main subjects studied in this paper. Obtained in the Material Analysis laboratory at Tetra Pak® in Lund [23]. The internal fibers of the paperboard material can be clearly seen in the figures. On top of Figure 2.3 there is the thin clay coat layer used for creating an even flat surface suitable for printing the graphics.

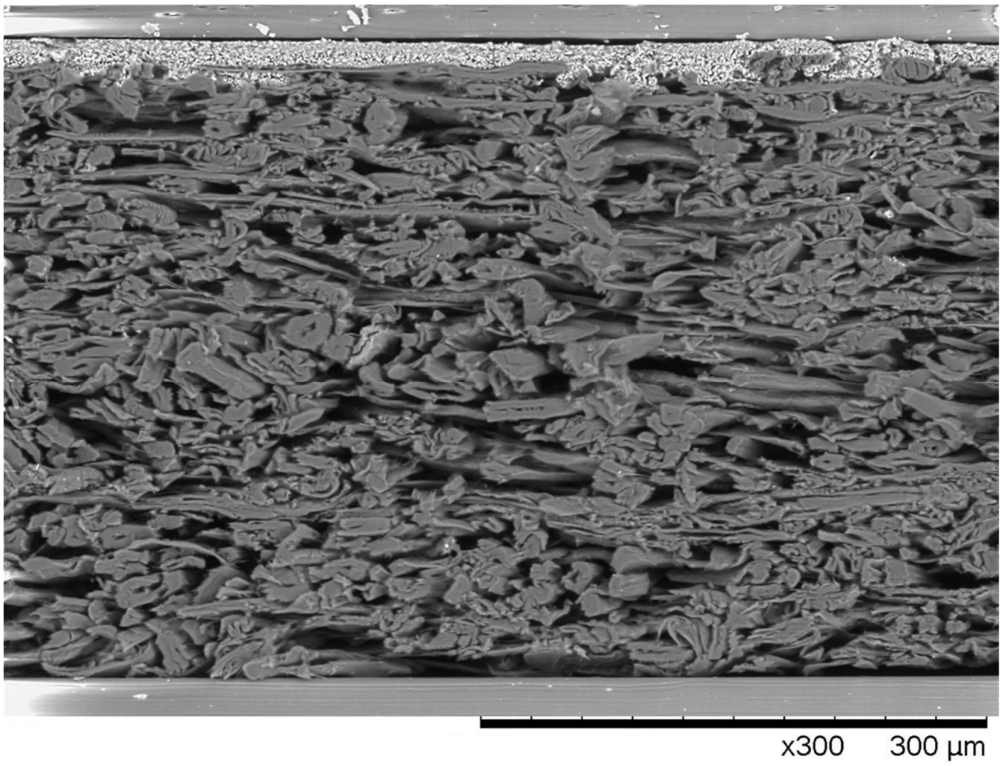

Figure 2.3: *SEM-picture of paperboard used in the TBA-packages[22]*

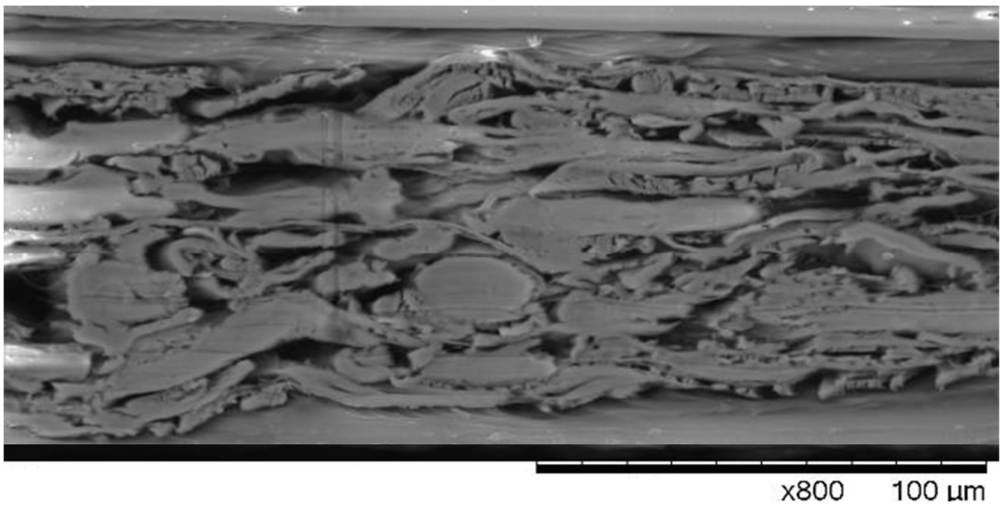

Figure 2.4: *SEM-picture of paperboard used in the TFA-packages[23]*

2.2.2. Mechanical properties of paperboard

Important properties of paperboard include: basis weight, thickness, density, volume, stiffness, bending, ply bonding and glueability. These properties are interrelated to varying degrees and are influenced by the ratio of virgin to recycled fibers and production conditions. This project focuses on the mechanical properties of paperboard, including yield strength, strain and Young's modulus, and their dependence on strain rate, which has a great impact on the production and

application of the package material.

Paperboard consists of lightweight cellulose fibers arranged in a distribution to stacked fiber planes. Depending on the paperboard, the fiber length ranges from 0.5-5 mm and the fiber diameter from 10-50 µm. The longer and thinner the fibers are, the less stiff the paperboard will be. This fiber, like glass and carbon fiber, has a high tensile strength.

The anisotropy of the paperboard material results from the manufacturing process in which the fibers are sprayed continuously along the manufacturing direction (i.e., the machine direction MD). The Cross-machine dimensions of the fibers are represented as CD, and together they are regarded as the in-plane dimensions of the paperboard. Perpendicular to the in-plane dimensions is the out-of-plane stacking direction of the fibers, denoted by ZD. The three reference directions of paperboard are illustrated in Figure 2.5. The elastic modulus in MD is usually 2-3 times higher than in CD and about 100 times higher than in ZD.**Error! Reference source not found.** The anisotropy of paperboard is defined by two characteristic directions, MD and CD.

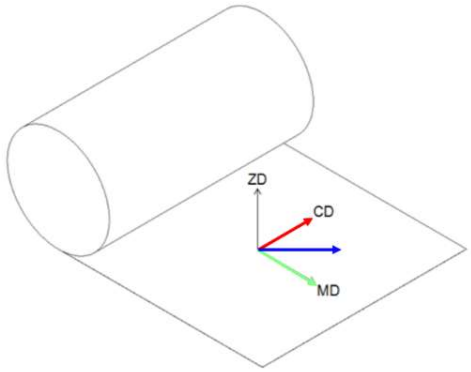

Figure 2.5: *The orientation of the three mutually-orthogonal material axes; Machine Direction (MD), Cross-machine Direction (CD) and out-of-plane direction (ZD).[2]*

Strain rate is the change in the strain of a material over time

$$\dot{\epsilon}(t) = \frac{d\epsilon}{dt} = \frac{d}{dt}\left(\frac{L(t)-L_0}{L_0}\right) = \frac{1}{L_0}\frac{dL(t)}{dt} = \frac{v(t)}{L_0} \qquad \textbf{Eq. 1}$$

where L_0 is the original length and L(t) its length at each time t, v(t) is the speed at which the ends are moving away from each other.

The strain rate at a point in the material measures the rate at which the distance between adjacent blocks of material near that point changes with time. It includes both the rate at which a material expands or contracts and the rate at which it deforms by progressive shearing without changing its volume. Figure 2.6 shows approximate division of strain rate regimes (in s^{-1}) and the experiments used to investigate these regimes.

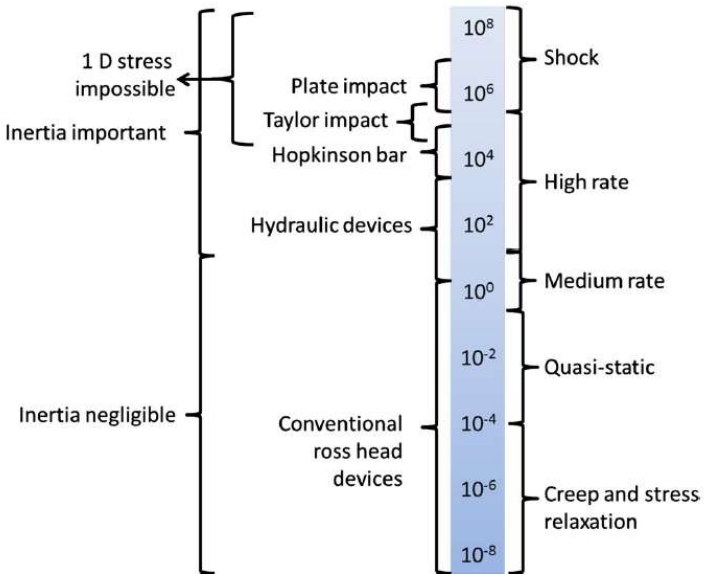

Figure 2.6: *Approximate division of strain rate regimes (in s^{-1}) and the experiments used to investigate these regimes.* [7]

From the literature review it was found the strain rate has a great effect on the surface roughening that an increased strain rate led to a more reduced surface roughness. This is because as the strain rate increases, more slip systems are activated and the roughness decreases.

Dynamic tensile tests show that at higher elongation rates, the paperboard layer usually behaves harder, especially with higher plastic stress-strain, fracture strength and relatively more initial yield stress.

2.2.3. Effect of strain rate on the mechanical properties of paperboard

During the manufacturing of the packaging material i.e. the converting process in the packaging material factories including creasing, lamination, and slitting with trimming of the packaging material the paperboard material is exerted to high magnitudes of strain rates. For example, the Tetra Pak® E3/CompactFlex chilled portion pack machine used to pack TBA has achieved a packing speed of 9,000 packages per hour.

Moreover, in the filling machine where tube forming, filling and package forming plus final folding occurs is another example where high speed is presented. Drop testing of the package and finally cutting and folding of paper straws, the material may be stressed and deformed at high strain rates, so the study about effect of strain rate on the mechanical properties is necessary. The operations in application and corresponding strain rates are shown in Figure 2.7 and Figure 2.8. The filling machine is shown in Figure 2.9.

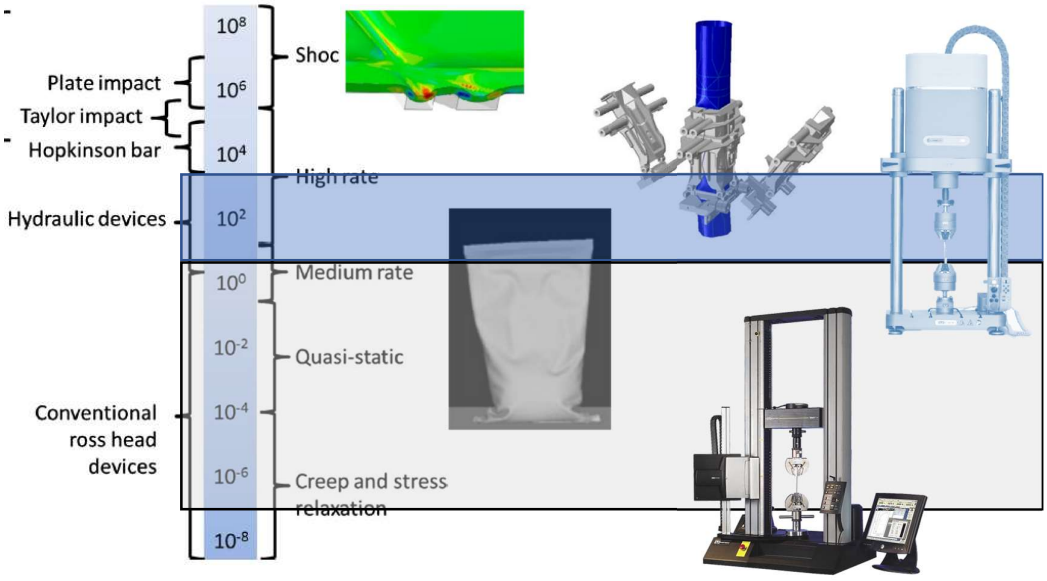

Figure 2.7: *Operations in application and corresponding strain rates[8]*

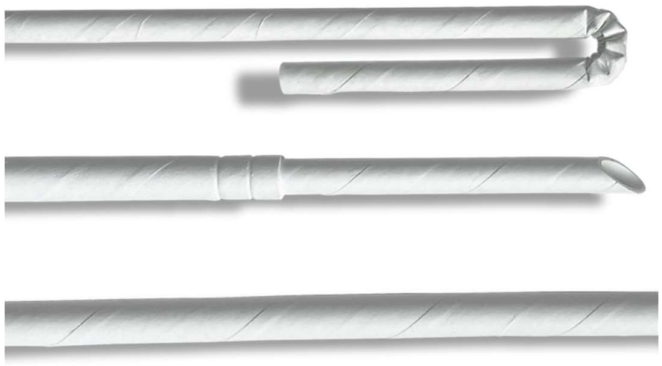

Figure 2.8: *Folding and pressing of paper straws*

Figure 2.9: *Tetra Pak® E3/CompactFlex high-speed filling machine[17]*

This chapter mainly investigates the force, stress and strain of paperboard material under different strain rates. As is introduced in Section 2.2.2, the anisotropy of paperboard is defined by two characteristic directions, so most rate-dependent responses along the MD, CD, and 45-degree directions are then tested.

Yu et al. summarized experimental data for metals, brittle materials and polymers in the low, medium and high strain rate ranges as presented in Figure 2.10[14]. Through their study, it was found that the dynamic strength or yield stress of the various materials had similar patterns. In the low and high strain rate range stresses are not strain rate sensitive. However, in the medium strain rate range, the dynamic strength or yield stress of these materials is extremely sensitive to the strain rate. This study has provided the basis for my subsequent research.

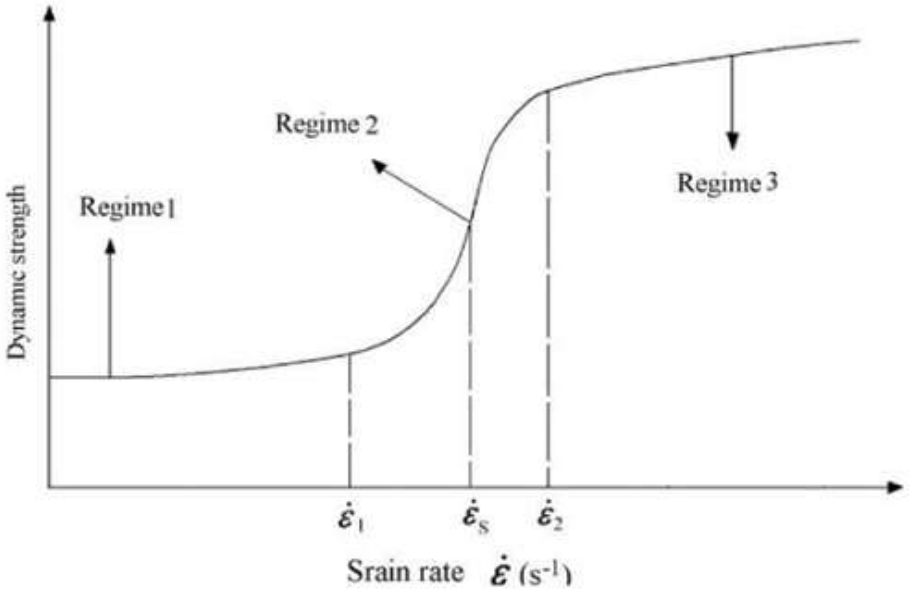

Figure 2.10: *Dependence of dynamical strength on strain-rates of engineering materials[14]*

A material similar to the paperboard used by Tetra Pak® was tested by Lian and summarized in Table 2.1[13]. The samples were tested at the strain rate from 0.0001 s^{-1} to 100 s^{-1}.

Table 2.1: *Stress and Strain at different strain rate of composite paperboard[13]*

Strain rate (s^{-1})	Stress (MPa)	Strain (mm/mm)
0.0001	17	0.013
0.001	18	0.013
0.01	20	0.013
1	22	0.016
10	28	0.018
100	45	0.020

Lian has only conducted experiments in one direction, but it can be seen from the data that stress, Young's modulus and strain rate show a significant positive correlation. Strain remains largely constant at lower strain rates and is also positively correlated at higher strain rates.

Robertsson considered three different strain rates for both in-plane and out-of-plane[2]. From his experiments and simulation which is concluded in Table 2.2, it can be found that at the initial stage of deformation, that is, the elastic deformation stage, the behavior of each strain rate is basically the same. The initial yield stress of paperboard is almost not affected by the strain rate, while the plasticity is affected by the strain rate. And the failure stress and strain are summarized in Table 2.3. There is a positive correlation between stress and strain rate and the failure stresses in the directions of MD, 45° and CD decrease successively.

Table 2.2: *Different strain rates during in-plane and out-of-plane tension.[2]*

	strain rate[1/s]	MD		45°		CD	
		stress [MPa]	Strain [%]	stress [MPa]	Strain [%]	stress [MPa]	Strain [%]
In-plane tension	1.67e-3	38	1.7	26	2.5	18	3.5
	1.67e-2	43	1.7	31	2.5	21	3.5
	1.67e-1	48	1.7	36	2.5	23	3.5
	strain rate[1/s]	stress [MPa]	Strain [%]				
Out-of plane tension	0.1	0.35	7				
	1	0.42	7				
	10	0.47	7				

Giashi**Error! Reference source not found.** studied three different layers of paperboard under higher strain rates and his research (Table 2.3 and 2.4) shows similar results to Robertsson's.

Table 2.3: *Comparison between top, middle and bottom layer.[3]*

strain rate [1/s]	top		mid		bottom	
	stress [MPa]	Strain [%]	stress [MPa]	Strain [%]	stress [MPa]	Strain [%]
0.06	65	2.5	30	1.9	43	2.4
10	/	/	32	1.8	50	1.7
20	77	2.2	37	1.6	62	2.1
40	82	2.1	42	1.8	70	1.7

Table 2.4: *Preliminary dynamic test results for full paperboard laminates in MD (Width 50mm, thickness 400μm) [3]*

strain rate (1/s)	0.06	20	40	60	70	80
Stress (MPa)	16.7	19.2	22	20.5	23.7	25
strain (%)	2.5	1.6	2	1.8	1.8	2.6

But Giashi's study at strain rates higher than 500 (1/s) have a violent oscillations and unreliable values. Following experiments in this paper will focus on the mechanical properties of materials at strain rates between 0.0167 s^{-1} to 16.7 s^{-1}.

In Allaoui's article[6] (Table 2.5), corrugated paperboard of three layers is tested with strain rate range going from 6×10^{-5} s^{-1} to 12×10^{-3} s^{-1}. This further confirms the existence of viscoelastic phenomenon in the linear part and viscoplasticity phenomenon in the nonlinear part.

Table 2.5: *Evolution of the failure stress (MPa) according to strain rate request[7]*

Direction		Strain rates (s^{-1})					
		6×10^{-5}	12×10^{-5}	6×10^{-4}	6×10^{-4}	6×10^{-3}	12×10^{-3}
Recto	σf (MPa) MD	36.24	35.94	42.77	42.03	43.01	45.27
	σf (MPa) CD	14.72	15.77	17.09	16.95	17.28	17.949
Verso	σf (MPa) MD	36.02	40.51	41.61	43.01	44.24	43.86
	σf (MPa) CD	15.15	15.86	16.42	17.85	18.02	19.76
Well	σf (MPa) MD	41.02	42.35	45.61	46.83	46.12	48.97
	σf (MPa) CD	15.83	16.24	16.67	17.52	18.82	18.83

Meanwhile, in the study of polymer packaging materials (Figure 2.11) it's found that the yield stress of (a) PMMA, (b)PC, (c) PVC, and (d) epoxy varied greatly at different strain rates but the yield strain is almost the same as paperboard. PMMA has the highest peak stress at most strain rates and all polymers have similar failure strain at peak and fracture.

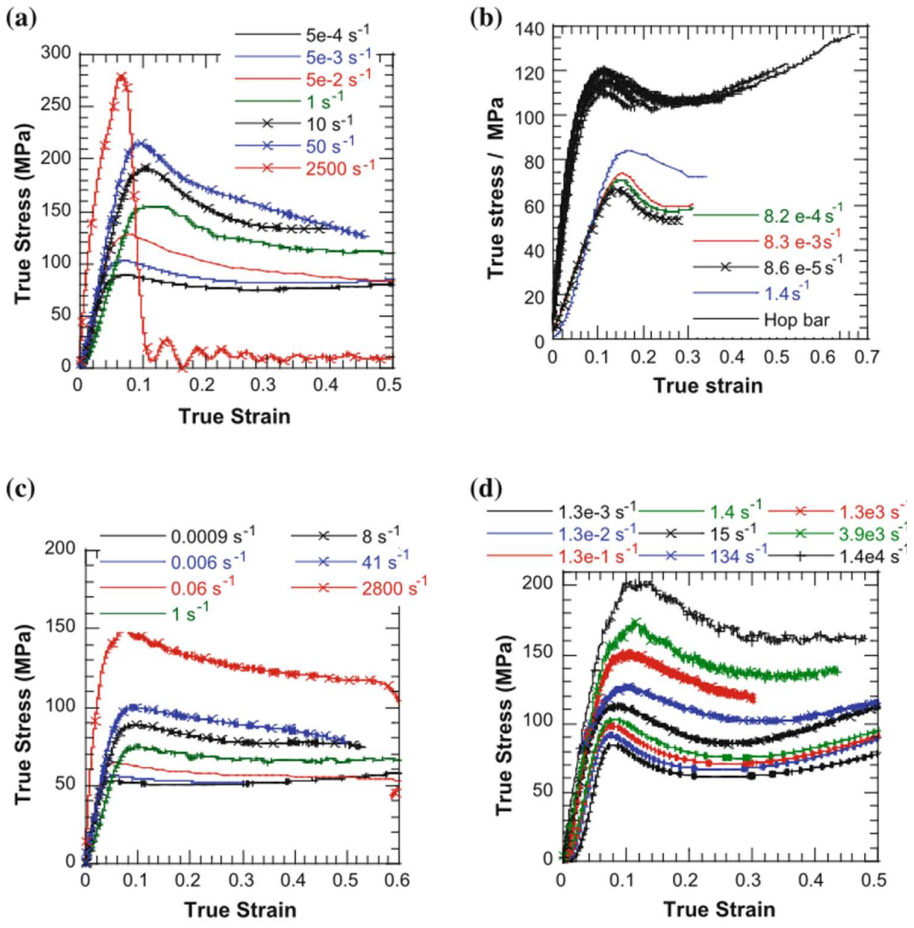

Figure 2.11: *Representative compressive stress–strain curves for (a) PMMA, (b)PC, (c) PVC, and (d) epoxy across a range of strain rates[7]*

Furthermore, the test results of aluminum foil (Table 2.6) show that strain rate has little effect on the failure stress and strain of the material in all directions. Experiments were carried out at three strain rates of 120 mm/s, 300 mm/s and 6000 mm/s.[8]

Table 2.6: *Result of tensile test for aluminum foil.*

RD		**TD**		**45°**	
stress [MPa]	**Strain [%]**	**stress [MPa]**	**Strain [%]**	**stress [MPa]**	**Strain [%]**
10	4.1	8.6	4	9	7.3

Besides experiment, researchers also developed simulation method for analysis. Borgqvist et al.[9] developed an elastoplastic 3D continuous model of paperboard shown in Figure 2.12. Simulation-driven product development can be carried out effectively with this model. A user material routine implementation of the model is implemented in Abaqus and LS-DYNA, and it is currently being used in research projects in industry. Model is used to simulate laboratory indents using linear crease tools and industrial rotary crease tools in 3D; the model is also used in molding simulations in a filling machine to identify machine-material interaction between different design parameters of the machine and the packaging material.

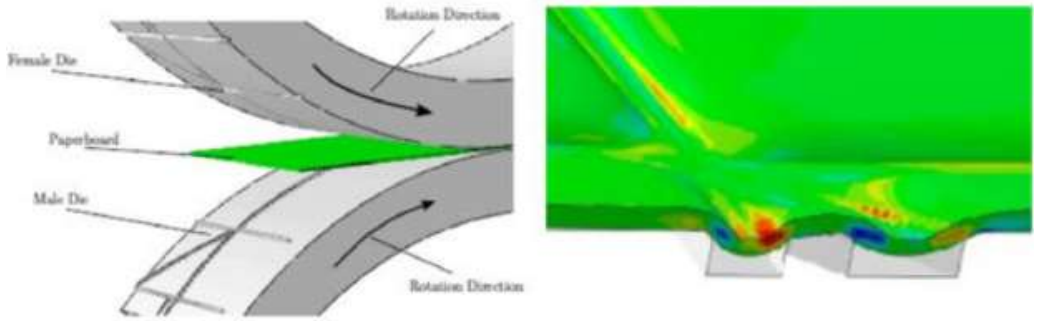

Figure 2.12: *Simulation of crease formation[9]*

Robertsson has developed an approach for combining the Borgqvist's model with solid shell finite elements and developed it specifically for predicting complex anisotropic materials (Figure 2.13). In comparison to a traditional approach, this element allows the modeling of regions with simple local deformation at a fraction of the cost. It was demonstrated that this approach allows detection of wrinkles, strain localization, and unwanted buckling in a full folding process including creases. Using these approaches, this project will enable simulations of real production scenarios that can be applied to industry.[9]

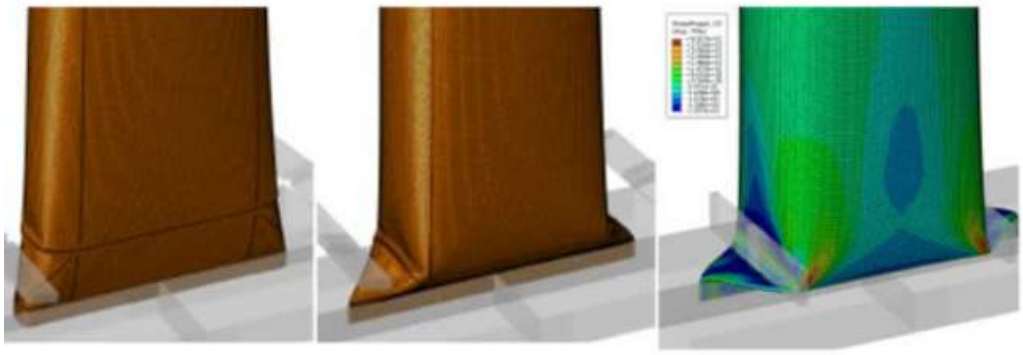

Figure 2.13: *Full forming simulation[10]*

2.3. Experiment methods for the analysis of structure-property relationship

In the study of materials, especially paperboard, optical microscopy and tensile testing are two commonly used in industry tools, as evidenced by the literature on this subject. Therefore, a brief description of their principles and how they usually work is given here.

2.3.1. Optical microscopy

Microscopy is the use of convex lens magnification imaging principle when human eye cannot resolve tiny object. Its main purpose is to increase the tiny object to the eye's angle of magnification (perspective of large objects in the retina imaging), with angular magnification M that their magnification capabilities. Because the same object to the eye angle of tension and the object from the eye distance, so generally specified like the distance from the eye at the magnification of 25 cm for the instrument magnification. The angle of view of a microscope is usually very small when observing an object, so the ratio of the angle of view can be replaced by the ratio of its tangent. Figure 2.14 shows the schematic of a wide-field optical microscope including an illustration of light rays from the light source to the detector.

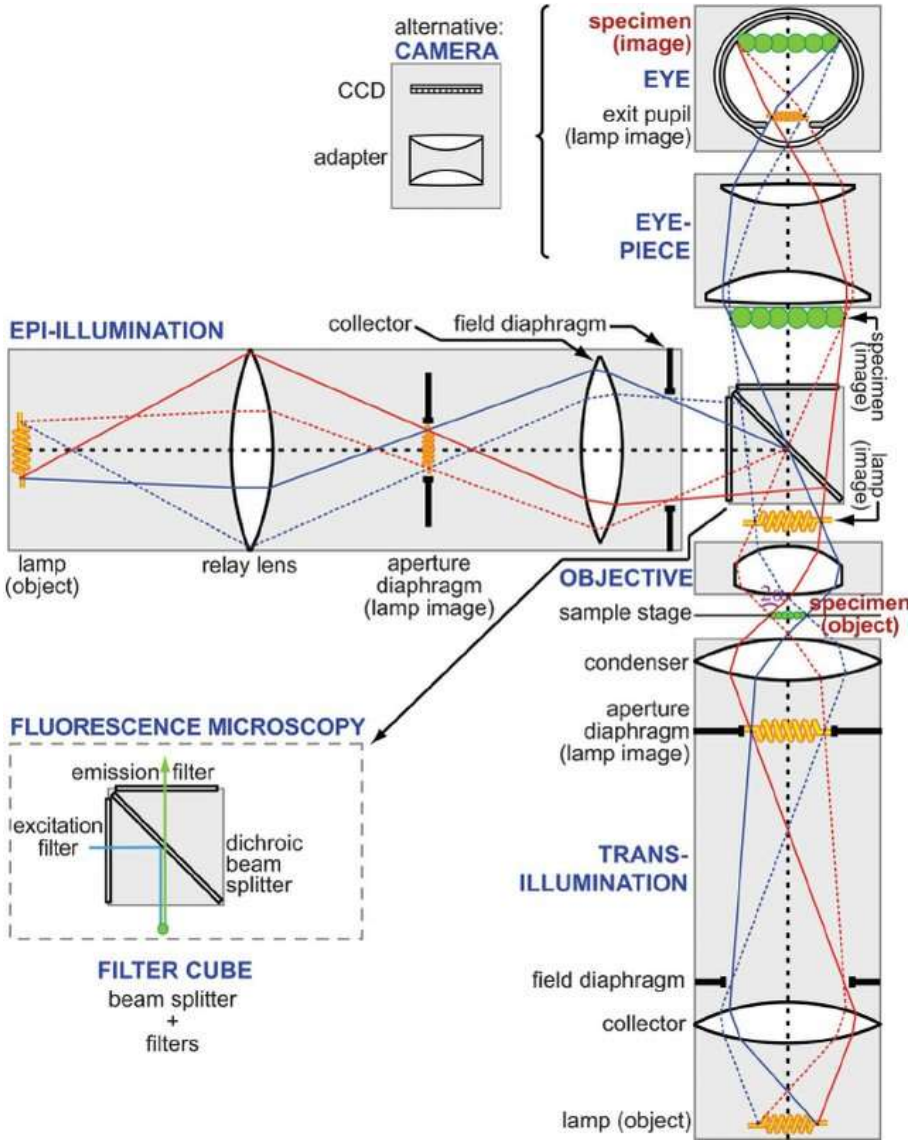

Figure 2.14: *Schematic of a wide-field optical microscope[21]*

In materials research, an optical microscope can display the microstructure of a material for observation. For example, metallographic organization of metal, fiber organization of paperboard, etc. With the help of modern advanced optical microscopes, panoramic images of materials and 3D surface reconstructions can also be obtained with software. This is very beneficial for studying the microstructure of materials. By obtaining the microscopic shape of the material, combined with other experimental data and theory, some properties of the material and the mechanism behind them can be discovered by researchers. Figure 2.15 shows a typical optical microscope used in research.

Figure 2.15: *Keyence VHX-6000 optical microscope 3D surface reconstruction schematic[19]*

2.3.2. Tensile testing

Tensile testing is a method for determining the properties of a material under an uni-axial tensile load. The results of the test depend on the shape and size of the specimen, the clamping method and the test method. The data obtained from tensile tests can be used to determine the elastic limit, elongation, modulus of elasticity, proportional limit, area reduction, tensile strength, yield point, yield strength and other tensile property indices of the material. Creep data can be obtained from tensile tests performed at high temperatures. A typical stress-strain curve is shown in figure 2.16. The most commonly used equipment in material mechanics experiments is the universal material testing machine, which can perform tensile, compression, shear, bending and other tests.

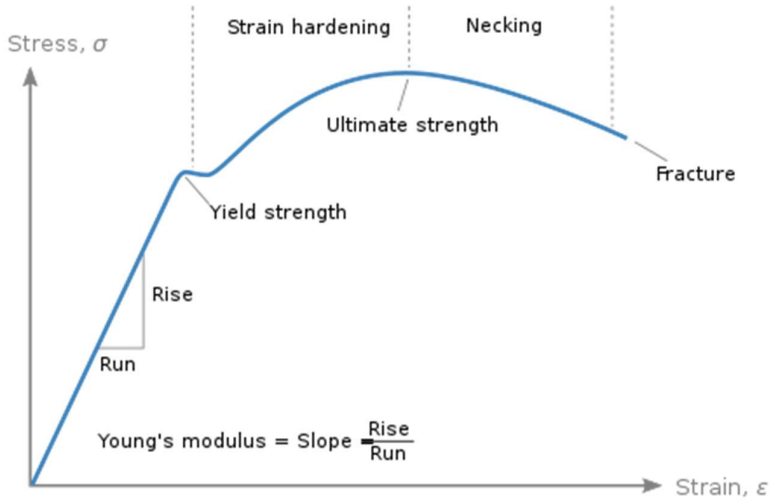

Figure 2.16: *Typical stress-strain curve[24]*

The most commonly used test is the uniaxial tensile test (load applied along the central axis), in which the specimen is stretched uniformly at a specified rate and the tensile and elongation are recorded. Material parameters such as stress-strain curve, yield strength, tensile strength and elongation at break are deduced. In addition, biaxial tensile tests are available.

Tensile testing machine is widely used in measurement and quality inspection; machinery manufacturing; packaging materials and food; petrochemical and other industries. Tensile jig as an important part of the instrument, different materials require different jigs, but also whether the test can be carried out smoothly and the accuracy of the test results is an important factor. Tensile testing machine is commonly used in all kinds of metal, rubber and plastic, textile and other types of materials.

With the data obtained from tensile tests, we can analyze the relationship and variation patterns between different properties of materials, such as stress-strain, yield strength-strain rate, etc., to determine how the material will work in various states of use. It is also possible to predict the material properties when the experimental conditions are not achieved based on the variation rule of the data, together with mathematical simulations. Figure 2.17 demonstrates the machine and schematic diagram of the principle for the experince.

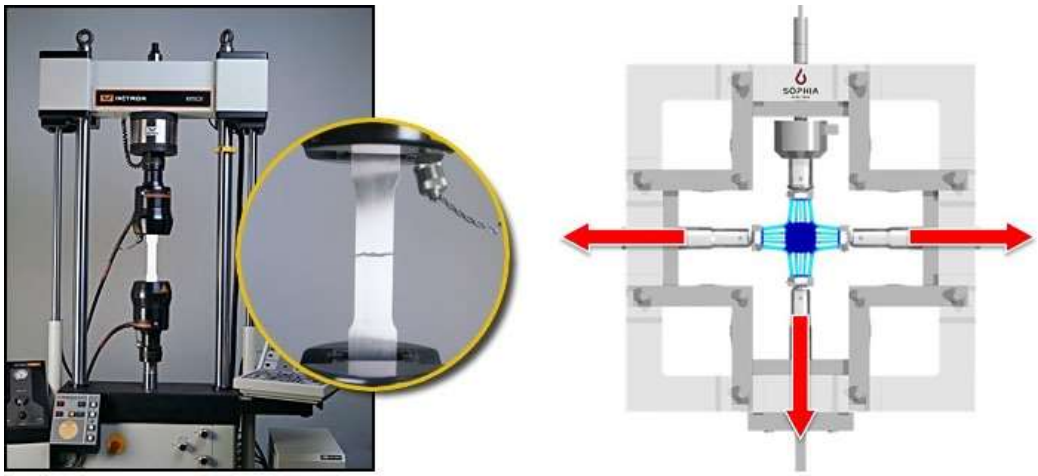

Figure 2.17: *Uniaxial tensile test and biaxial tensile test[20]*

3. Materials and experimental methods

In this chapter, the materials and experimental methods of the study are described in detail. Material samples were provided by Tetra Pak® and the experiments were mainly carried out at LTH.

3.1. Paperboard materials of interest in packaging materials

The first experimental material is a thin paperboard utilized in a "pillow"-shaped package format called TFA, Tetra Fino® Aseptic (Figure 3.1 a)[1]. From the outside, these packages look simple, but the process of manufacturing them is complex. First, a continuous roll of carton packaging material is fed into a filling machine and sterilized. The material is formed and sealed into a tube and filled, allowing it to expand. It is then shaped and sealed to maintain sterility. Finally, it is cut into individual packs. The product is filled in Tetra Pak® A1[11] and is sealed at a high strain rate, therefore, it is important that mechanical properties are tested at different strain rates for this product.

As-supplied paperboard sheets were cut by a paper cutter into strips 100 mm long and 15 mm wide (Figure 3.1 b)) for MD and CD respectively according to ASTM D828 for testing. The thickness of the sample was measured at 101 μm. The clamping areas were covered by masking tape in order to prevent samples from being damaged by grips.

Figure 3.1: *a) Tetra Fino® Aseptic[1]; b) Sample size and shape description*

The second experiment material Tetra Brik® Aseptic (TBA) paperboard, which is shown in figure 3.2 the same as Robertsson[2] tested. This material was tested at higher strain rates than Robertsson's experiment but only cut along MD (the same size and shape as TFA material with thickness of 410 μm).

Figure 3.2: *Tetra Brik® Aseptic[1]*

3.2. Mechanical testing

ElectroPuls® E10000 Linear-Torsion with ±10 kN force and ±100 Nm torque capacity is used for obtaining information on the mechanical properties of material. From the tests, strain rate, young's modulus, load at yield, tensile stress at yield, maximum load, tensile stress at maximum load, tensile strain at maximum load can be obtained. These data are used as a background for the analysis of material performance at high strain rates.

Designed for dynamic and static testing of a broad range of materials and components, it is a state-of-the-art, all-electric test instrument. It is powered by a single-phase supply and requires no additional utilities for basic operation (for example, air, hydraulics, or water).

Load Frame + Base Unit incorporating:
- Electric Linear Actuator
- Linear Load Cell
- Linear Absolute Encoder - Cooling System (in base unit)
- Linear Power Amplifier (in base unit)

Linear - Torsion Load Frames also incorporate:
- Electric Rotary Actuator
- Biaxial Load Cell
- Rotary Absolute Encoder
- Rotary Power Amplifier (in controller)

Figure 3.3: *ElectroPuls® E10000 Linear-Torsion*

The highest speed of this equipment is 20m/s, which can meet the experimental requirements of strain rate of 80/s.**Error! Reference source not found.**

It includes Instron® advanced digital control electronics, bi-axial Dynacell™ load cell, Console software, and the very latest in testing technology – hassle-free tuning based on specimen stiffness, electrically operated crosshead lifts, a T-slot table for flexible test set ups and a host of other user-orientated features.

To obtain information on the mechanical properties of the materials at different strain rates, I tested samples of the material in LTH using an Instron E10000 experiment machine. This tensile test is uniaxial, i.e. the force is applied along one axis. The uniaxial tensile test is the most common test method and is usually sufficient. The biaxial tensile test is usually used to test the anisotropy of a material, and this experiment achieves this by cutting the original material along the MD and CD and testing them separately. This will make the experiment simpler and reduce errors. Figure 3.4 shows the sketch of the basic components of the tensile testing machine used.

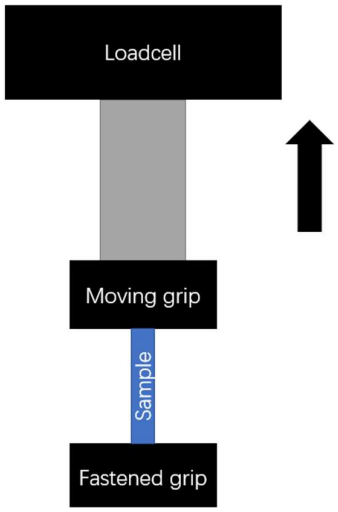

Figure 3.4: *The basic* components *of Uni-axial Tensile testing machine.*

To investigate the relationship between Young's modulus, tensile stress at maximum load, tensile strain at maximum load and strain rates, tensile tests were carried out from 0.0167 s^{-1}, to 1.67 s^{-1}. Each batch includes at least 3 specimens for MD and 3 specimens for CD. Due to the performance limitations of the experimental machine, the experiments could not be carried out properly at higher strain rates.

Uncontrolled movement of the sample may lead to errors in the experimental data. To ensure that there is no slippage between the sample and the grip, the sample was securely fixed and it was marked close to the grip. After the test it was determined whether sliding had occurred by checking whether movement had occurred at the mark. The reproducibility of the results in a batch is also one of the methods to determine whether an unpredictable problem has occurred with the operation and sample.

Whether a sample is stably stretched (i.e. elongation is linearly related to time) can be determined from the extension - time curve in Figure 3.5.

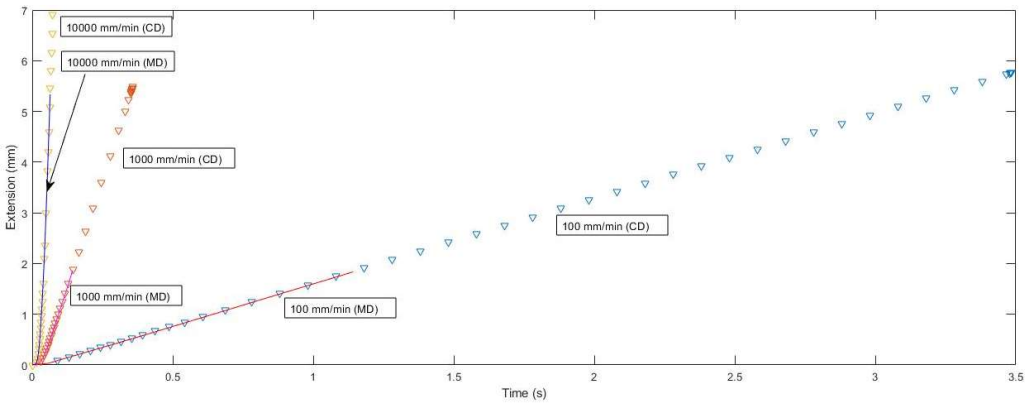

Figure 3.5: *Extension – time graph of each batch*

3.3. Optical microscopy

Keyence VHX-6000 (Figure 3.6) used in the experiment is an advanced digital optical microscope with light polarization, differential interference contrast, various reflected and transmitted light illumination options. Its High-End analog capacities are further reinforced with latest digital-world technology including camera, X-Y-Z ($40\times40\times49mm^3$) motorized stage and image processing allowing fast large-area panoramic imaging, 3D surface reconstruction and post-acquisition processing and quantification. The instrument chassis also allows 360° stage rotation and +60° / -90° eccentric camera tilt.

Samples of paperboard material tested in the tensile test at different strain rates were next observed under an optical microscope. The observation of fractures, fiber morphology, and wrinkles can help analyze the effect of strain rate on the mechanical properties of the material.

Figure 3.6: Digital optical microscope Keyence VHX-6000

4. Experimental results on the mechanical properties, microstructure, and fracture of paperboard

4.1. Mechanical testing of paperboard

Firstly, the similarities and differences between the two materials can be seen in their appearance. This leads to their different mechanical properties. Figures 4.1 and 4.2 below show images of each of the above materials under an optical microscope. As can be seen from the two different microscopic images, the fibers that make up the two materials, although different, are arranged relatively neatly in the same direction.

We can also see the difference in thickness between the two materials from the graphs that the thickness of TFA is approximately 100μm and the thickness of TBA is approximately 400μm. In addition, the fibers are arranged relatively tightly and the surface of the paperboard material is flat.

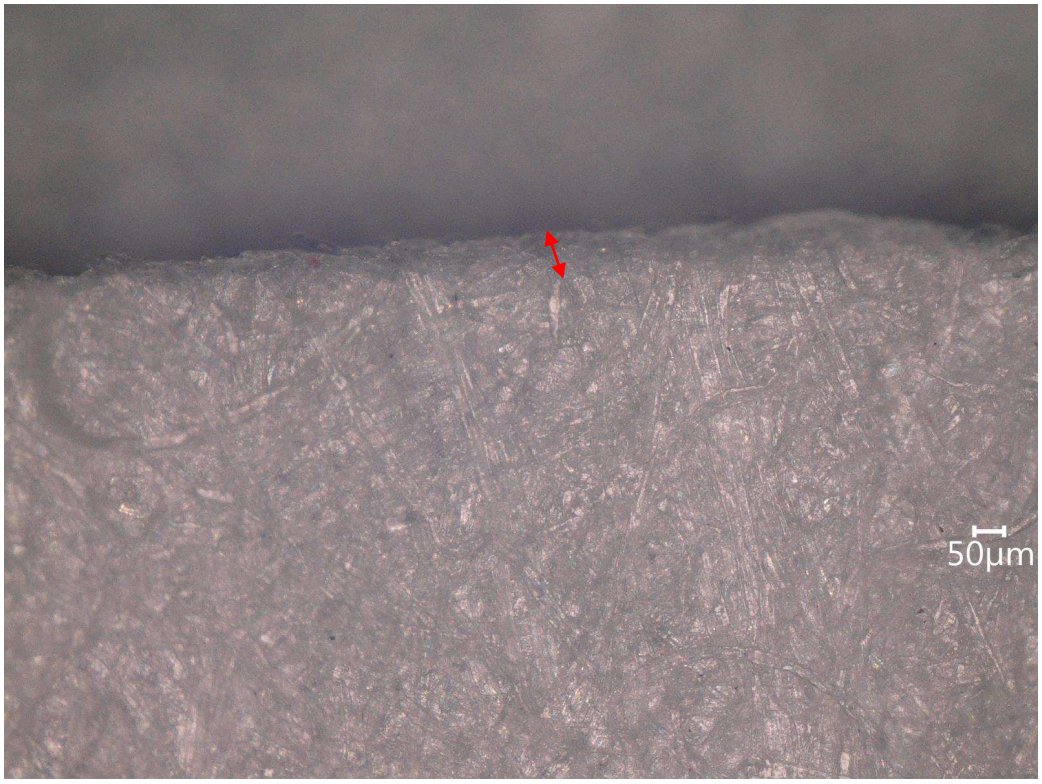

Figure 4.1: *Optical micrographs of TBA-material*

Figure 4.2: *Optical micrographs of TFA-material*

4.1.1. Effect of strain rate in mechanical testing of TFA material

As there is excellent reproducibility within each group of experiments, I selected the mean value of each group to plot in order to make the results more intuitive for TFA material. Figure 4.3 and 4.4 below show stress-strain curves from tensile tests of each batch.

The dependence of mechanical properties on strain rate in paperboards under investigation in the present study is non-monotonic. At high strain rates of $0.833s^{-1}$ and higher, the total elongation at failure of specimen is much larger than that at low strain rates. From this figure it's not so clear to see the relationship between yield stress and strain rate and the relationship curves for these two variables will be shown in later sections according to Table 4.1.

From Figure 4.4 similar results can be drawn. According to the summary of experimental data in Table 4.1, it is also known that the Young's modulus in both directions is independent on the strain rate. At all strain rates, the yield strength of the material is greater in MD while the strain in CD is greater.

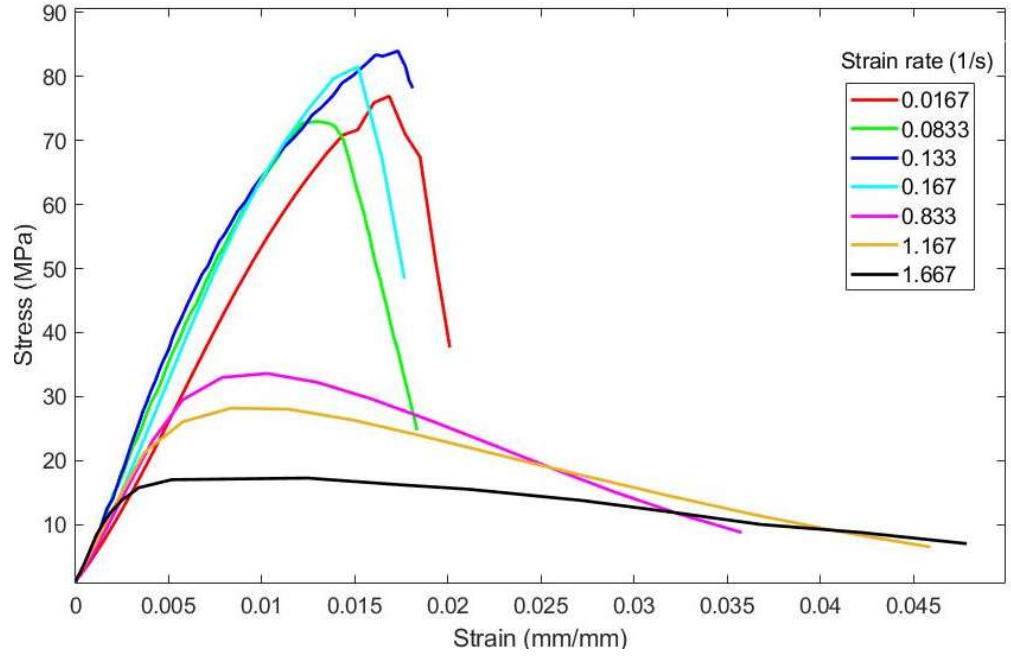

Figure 4.3: *Stress-strain curve for tensile tests of TFA in MD from 0.0167 s^{-1} to 1.67 s^{-1}*

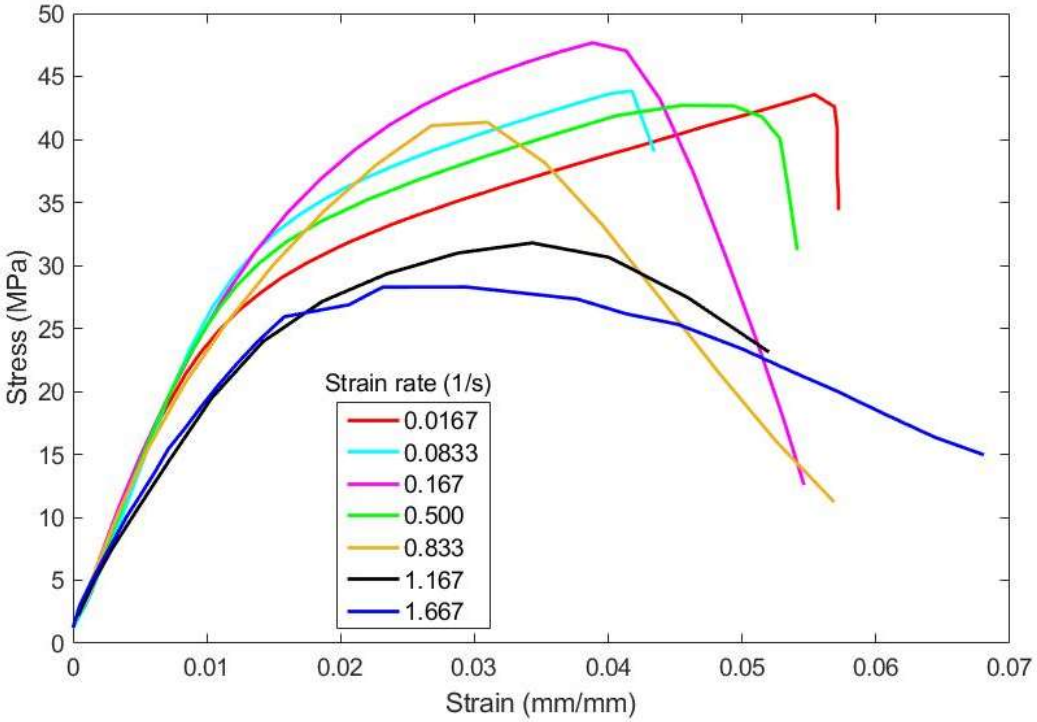

Figure 4.4: *Stress-strain curve for tensile tests of TFA in CD from 0.0167 s^{-1} to 1.67 s^{-1}*

Table 4.1: *Experimental results on mechanical properties for TFA material*

	Strain Rate	Young's Modulus	Load at Yield	Tensile stress at Yield	Maximum Load	Tensile stress at Maximum Load	Tensile strain at Maximum Load
Unit	s^{-1}	GPa	N	MPa	N	MPa	mm/mm
MD	0.0167	8.115	100.835	66.442	135.847	89.543	0.018
	0.0833	5.919	107.166	71.444	109.615	73.077	0.016
	0.167	7.236	107.723	71.816	113.117	75.412	0.013
	0.833	5.707	49.895	33.263	50.761	33.841	0.009
	1.17	5.733	39.157	26.105	41.203	27.469	0.009
	1.67	6.922	26.460	17.640	29.134	19.422	0.007
CD	0.0167	2.762	37.228	24.819	65.620	43.747	0.056
	0.0833	2.860	45.782	30.521	69.398	46.265	0.049
	0.167	2.750	42.164	28.110	66.583	44.388	0.048
	0.500	2.791	43.575	29.050	71.992	47.994	0.040
	0.833	2.711	35.998	23.999	62.606	41.738	0.028
	1.17	2.349	33.934	22.623	56.606	37.737	0.029
	1.67	2.426	26.066	17.377	46.042	30.694	0.022

4.1.2. Effect of strain rate in mechanical testing of TBA material

For TBA material, the same experiment method was used to test its properties in MD and the similar results can be drawn (Figure 4.5 and Table 4.2). At high strain rates of $1.167s^{-1}$ and higher, the elongation at failure of specimens is much larger than that at low strain rates. The yield strength and Young's modulus of TBA is lower than those in TFA.

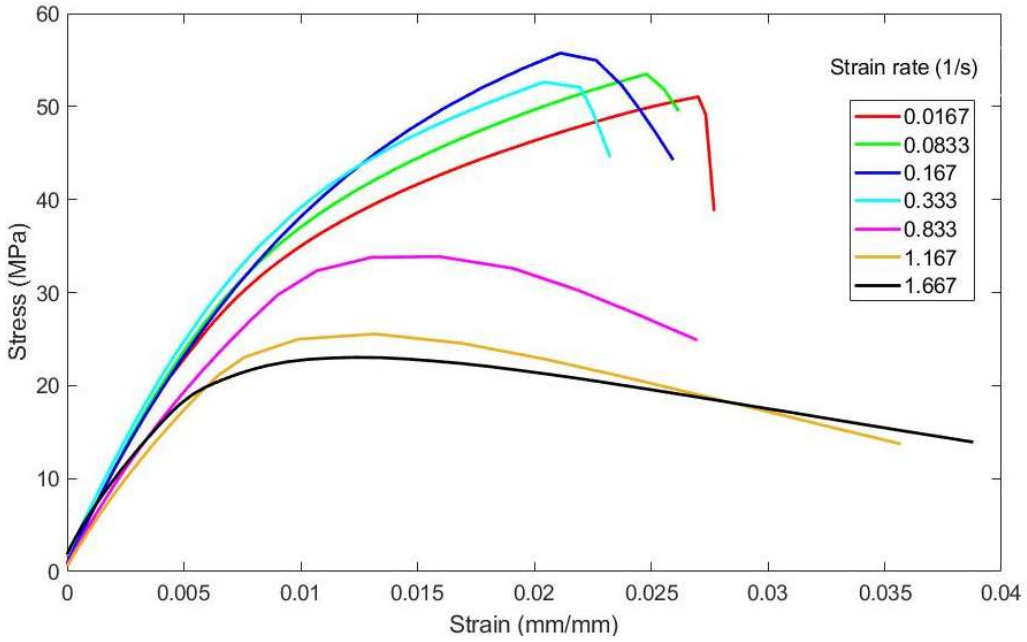

Figure 4.5: *Stress-strain curve for tensile tests of TBA material from 0.0167 s^{-1} to 1.67 s^{-1}*

Table 4.2: *Experimental results on mechanical properties for TBA material in MD*

	Strain Rate	**Young's Modulus**	**Load at Yield**	**Tensile stress at Yield**	**Maximum Load**	**Tensile stress at Maximum Load**	**Tensile strain at Maximum Load**
Unit	**s^{-1}**	**GPa**	**N**	**MPa**	**N**	**MPa**	**mm/mm**
	0.0167	4.865	198.742	32.316	316.793	51.511	0.027
	0.0833	5.153	206.503	33.578	331.923	53.971	0.026
	0.167	5.106	224.117	36.383	338.940	55.025	0.024
	0.333	5.046	214.467	34.873	344.951	56.090	0.022
	0.833	4.475	166.409	27.187	216.165	35.309	0.014
	1.17	4.120	139.901	22.748	157.454	25.602	0.012
	1.67	4.690	120.904	19.902	138.420	22.785	0.011

4.2. Analysis of microstructure in TFA and TBA paperboards

Figure 4.6 shows the TFA samples that had been tested in tension at different strain rates observed under an optical microscope. It can be seen from Figure 4.6 that the fibers at the fracture from 0.0833 s^{-1} to 1.67 s^{-1} gradually become aligned (same lengths). The fibers were significantly extended at a strain rate of *1.67 s^{-1}*. This explains the significant increase of strain in paperboard at high strain rates.

a) 0.0833 s^{-1} *b) 0.133 s^{-1}*

c) 0.167 s^{-1} *d) 1.67 s^{-1}*

Figure 4.6: *Microscopic images of TFA in MD at different strain rates*

The morphological changes of the fibers can be more clearly understood from Figure 4.7.

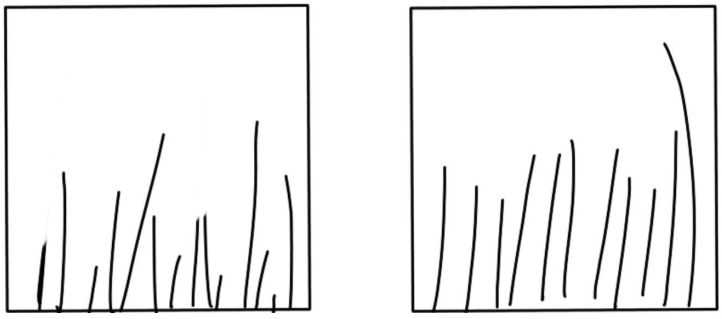

Figure 4.7: *Sketch of fibers after test along MD at strain rate of 0.0833 s^{-1} and 1.67s^{-1}*

In CD, less broken fiber can be seen and the fractures of the 0.0167 s^{-1} and 0.167 s^{-1} samples are uneven while the fibers of the 0.833 s^{-1} and 1.67 s^{-1} samples are looser (Figure 4.8). This is similar to the condition of MD.

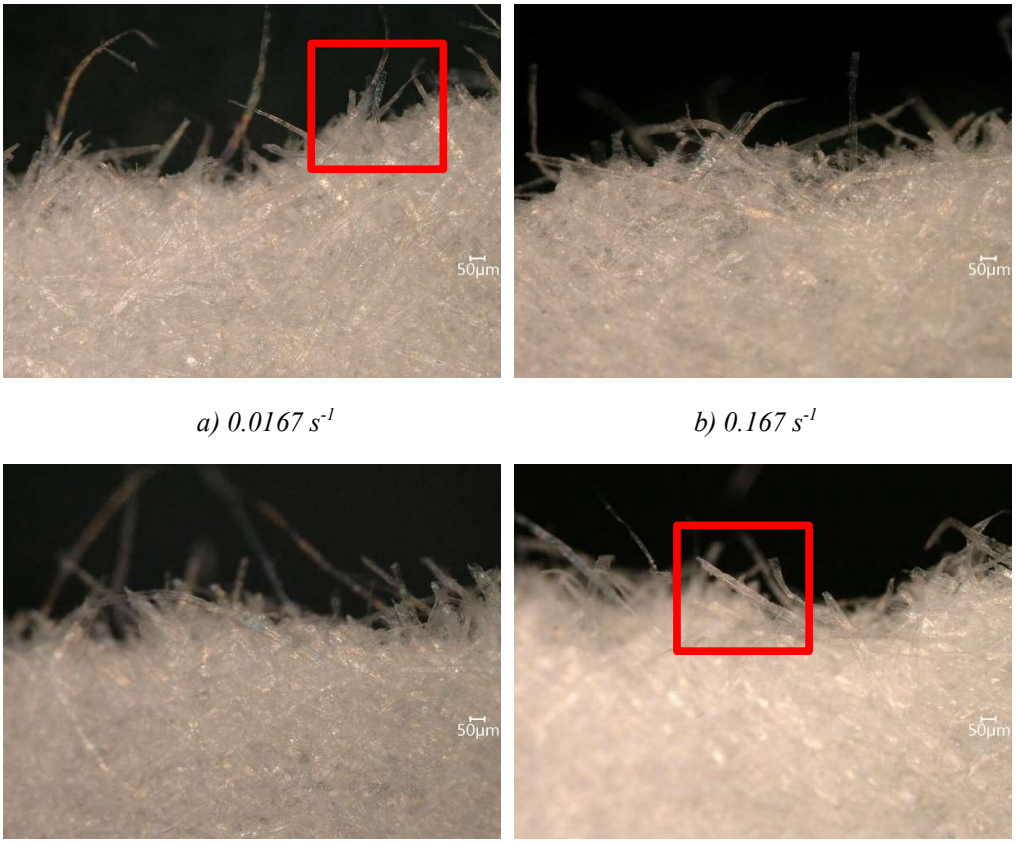

a) 0.0167 s^{-1} *b) 0.167 s^{-1}*

c) 0.833 s^{-1} *d) 1.67 s^{-1}*

Figure 4.8: *Microscopic images of TFA in CD at different strain rates*

The morphological changes of the fibers can be more clearly understood from Figure 4.9.

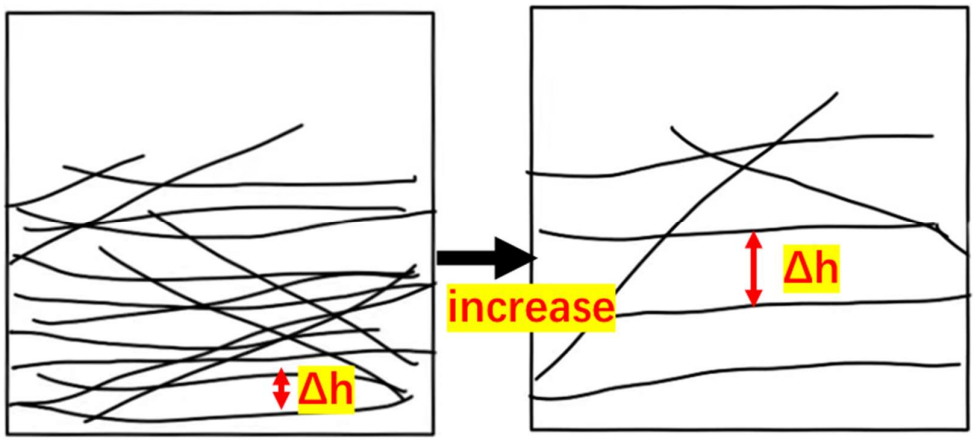

Figure 4.9: *Sketch of fibers after test along CD at strain rate of 0.0167 s^{-1} and 1.67s^{-1}*

The TBA material also had similar differences to those found above at the fracture of the samples at strain rates of 0.0167 s^{-1} and 1.67 s^{-1} (Figure 4.10). In addition, because the TBA material is relatively thick, obvious delamination can be seen in the tensile fracture at low strain rate.

a) 0.0167 s^{-1} *b) 1.67 s^{-1}*

Figure 4.10: *Microscopic images of TBA in MD at different strain rates*

3D images of the TFA material at the wrinkles resulting from stretching at *0.0167 s^{-1}* in Figure 4.11. It shows that the wrinkles in CD are deeper and more evident, which can also be seen in next section.

a) MD

b) CD

Figure 4.11: *3D microscopic images of TFA in MD and CD at 0.0167 s^{-1}*

For TBA samples, the wrinkles produced after stretching are less visible in appearance due to the thicker and stiffer samples themselves (darker areas is the wrinkle) which is shown in Figure 4.12.

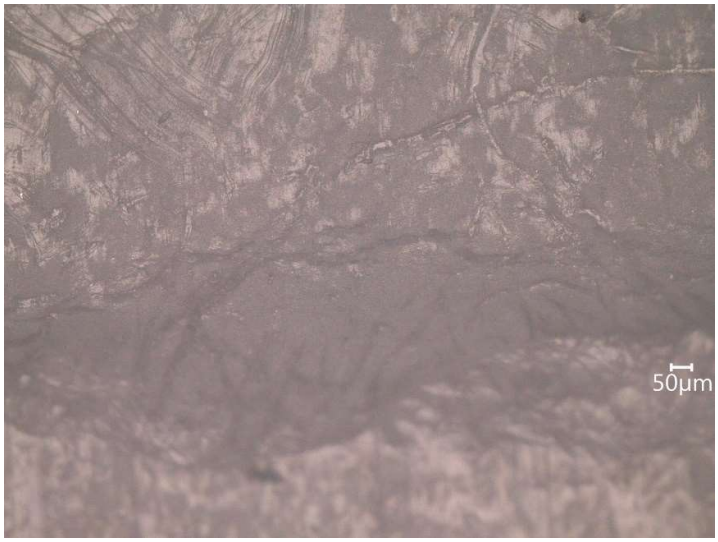

Figure 4.12: *3D microscopic images of TBA in MD at 1.67 s^{-1}*

4.3. Analysis of fracture in TFA and TBA paperboards

From Figure 4.13, the fracture of all samples occurred in the stretching area, rather than near the grips. The fractures are all essentially perpendicular to the direction of tension. At a strain rate of 0.0167 s^{-1}, the fracture of the sample is relatively rough, which is due to the fact that at low strain rate, the strain distribution is very uniform and the damage area of the specimen slowly expands toward the adjacent weakest point to form a rough fracture surface. In addition to the forces along the fibers, the fibers around the points that have broken are subjected to bending stresses perpendicular to them and therefore will be more easily damaged. At a strain rate of 1.67 s^{-1}, a relatively flat fracture can be observed, which is due to the rapid expansion of the damaged area of the specimen into fracture damage. This is common to both materials.

For TFA cut along the MD, the morphology of the sample after tensile testing at low strain rates of 0.0167 s^{-1} and 0.167 s^{-1} is virtually indistinguishable from that before stretching. This is also reflected in the fact that they have a small yield strain. This is because almost no deformation of the fibers takes place, except at the fracture.

The specimens tested at 1.67 s^{-1} have slight wrinkle in close to the area of contact with the grip.

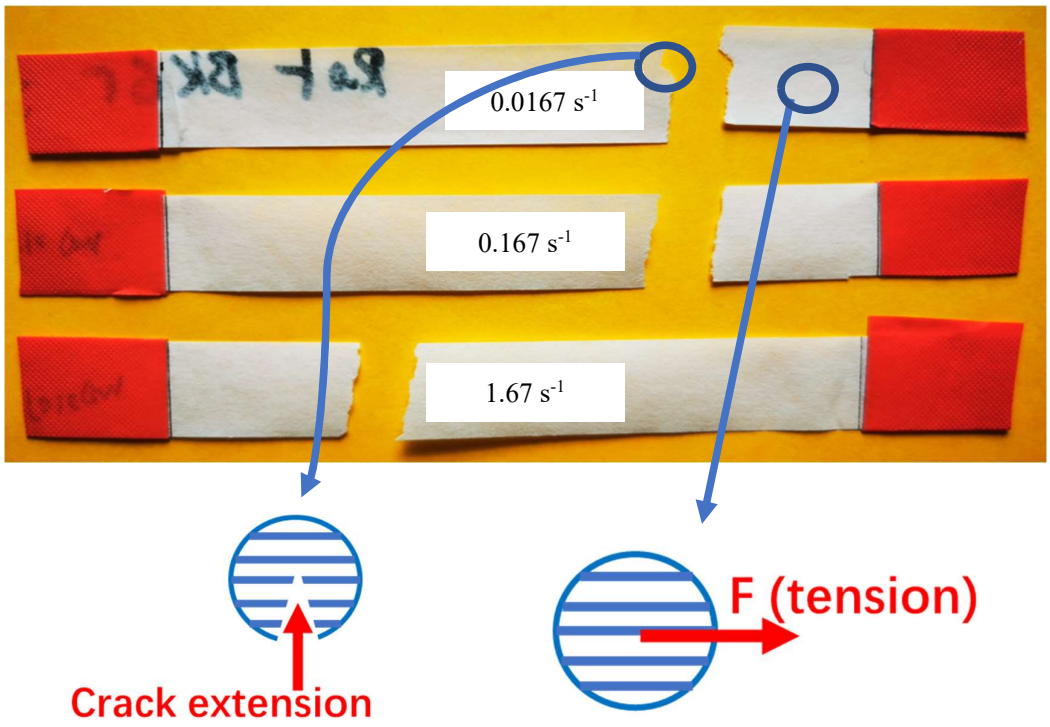

Figure 4.13: *Samples of TFA material cut along MD after the experiment*

For TFA cut along the CD (Figure 4.14), the samples tested at all three strain rates showed significant wrinkle, which became apparent as the strain rate increased. It can be assumed that this is due to the small number of fibers along this direction and the weak connections between the parallel fibers. These hydrogen bonds govern the behavior of paperboard in CD, which is less than the strength of cellulose fibers. As the parallel fibers become loose with stretching, the paperboard becomes thinner or even breaks when the few fibers that are used as a link break (Figure 4.15).

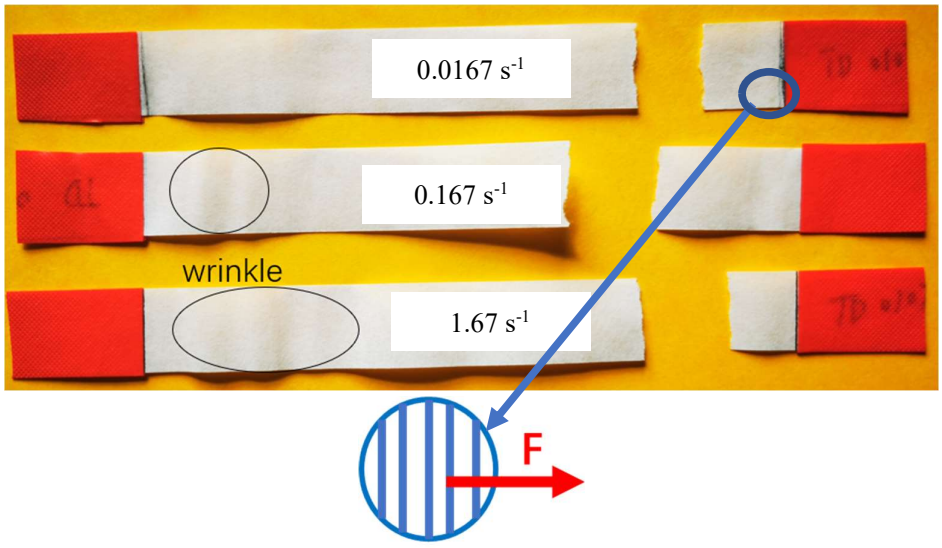

Figure 4.14: *Samples of TFA material cut along CD after the experiment*

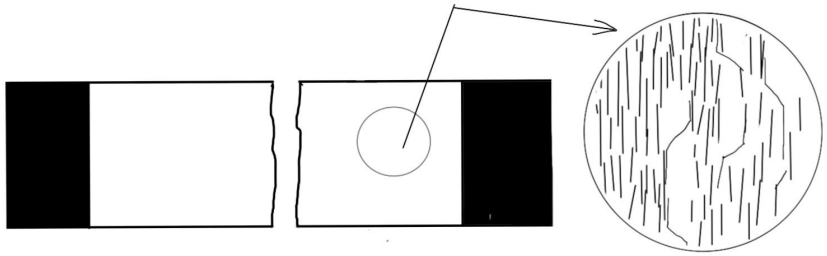

Figure 4.15: *Schematic diagram of the fiber arrangement in the wrinkle of TFA cut along CD*

The fracture of the TBA material at different strain rates is also basically perpendicular to the direction of force, but because the paperboard is thicker and consists of different layers, the fracture is not exactly perpendicular to ZD (Figure 4.16). Slight wrinkles appeared in the samples at all strain rates, and the number increased with increasing strain rate.

Figure 4.16: *Samples of TBA material after the experiment cut along MD*

The paperboard is made up of different layers, as shown in Figure 4.17.

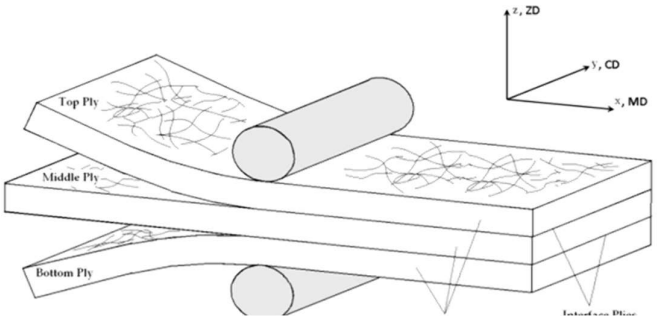

Figure 4.17: *Schematic diagram of layers in paperboard*

5. Analysis of structure-property relationship in paperboard materials

In this chapter, in order to study the relationship between paperboard material properties and structure, the relationship between yield strength, strain, Young's modulus and strain rate is used as the main object being studied.

The reason why the yield strength is chosen instead of the strength at the maximum loading is that the material occurs in elastic deformation at the beginning of deformation, and the deformation of paperboard in practical applications occurs within this range, and once this range is exceeded the material will fail. Therefore, the yield strength is more valuable in the study of the mechanical properties of materials.

5.1. Effect of strain on mechanical properties and fracture of TFA material

A diagram showing the relationship between yield stress and strain rate for TFA is presented in Figure 5.1.

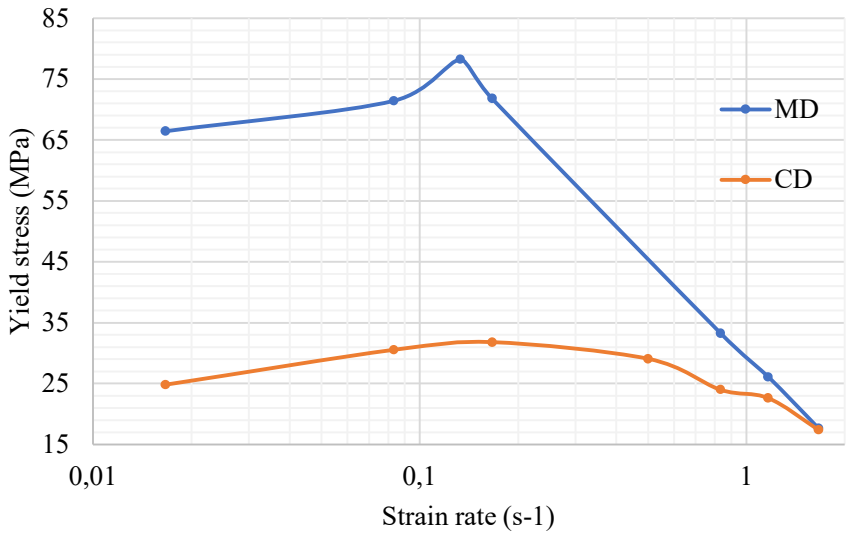

Figure 5.1: *Stress-Strain rate graph of TFA (The horizontal axis is logarithmic)*

According to this result, yield stress of material cut along MD is obviously higher than that in CD at all strain rates, i.e., the anisotropy of paperboard. This is due to the fact that the strength of the paper fibers themselves is greater than the strength of the connections between the fibers. This is also in line with previous speculations based on the arrangement of the fibers in the paperboard material.

This also explains the wrinkles (waves) that appear in the paper after stretching in Figure 5.2.

The disrupted areas between poorly connected fibers become thinner and the change in thickness causes wrinkles to develop. The morphology of the samples also varies between experimental conditions and different cutting orientations; this will be presented and discussed in the following section.

Figure 5.2: Wrinkles in *TFA sample after testing*

In both directions, the yield strength showed a trend of increasing and then decreasing, with the minimum value both occurring at 1.67 s^{-1}, and maximum values occurring at 0.133 s^{-1} (in MD) and 0.167 s^{-1} (in CD). For the strain at fracture, that in CD is higher than that in MD, and a positive correlation with the strain rate is basically shown in both directions according to Figure 4.3 and 4.4, which coincides with the macroscopic and microscopic images shown in the previous chapter.

In MD, in addition to the forces along the fiber direction, the fiber is also subjected to forces perpendicular to the fiber direction from the part that has been broken to the surrounding area. At lower strain rate of 0.0167 s^{-1} this force has sufficient time to act, i.e. the crack can expand, while as the strain rate increases to 0.133 s^{-1} it can be assumed that the fiber at the fracture is almost exclusively pulled by external forces and therefore has a high yield strength. With a further increase of the strain rate, the decrease of the yield strength cannot be explained for the time being.

No significant dependence of Young's modulus on strain rate was found in these cases.

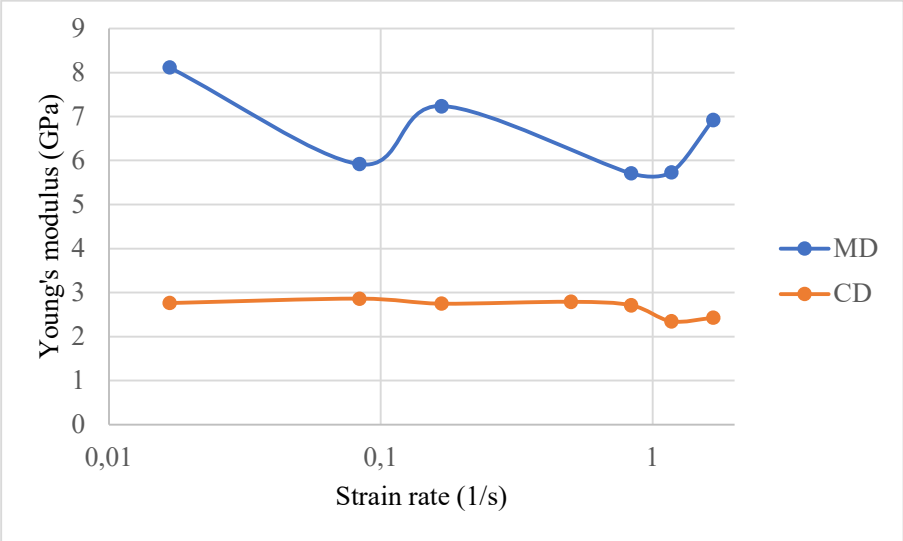

Figure 5.3: *Young's Modulus-Strain rate graph of TFA (The horizontal axis is logarithmic)*

5.2. Effect of strain on mechanical properties and fracture of TBA material

A graph can be plotted according to Table 4.1 which shows the relationship between yield stress and strain rate for TBA.

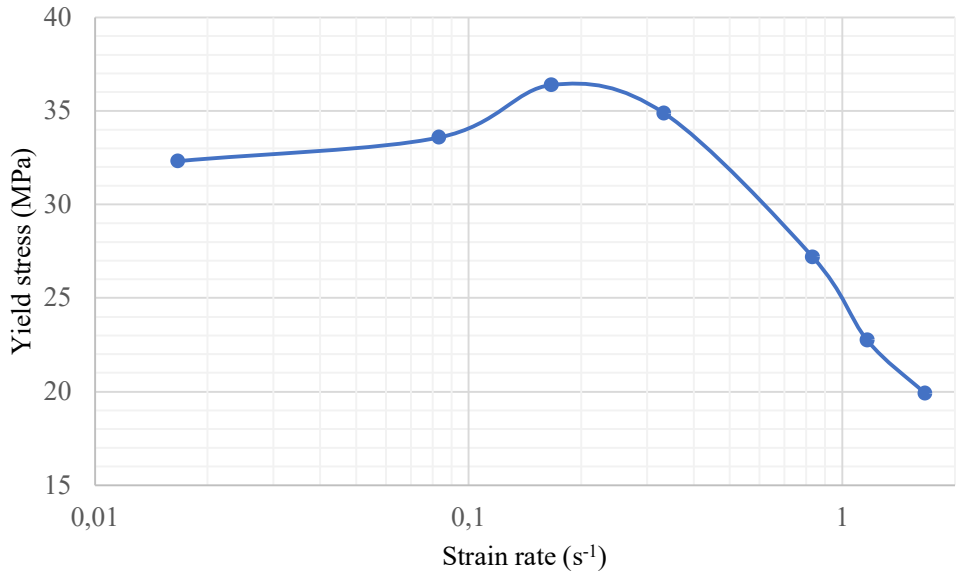

Figure 5.4: *Stress-Strain rate graph of TBA (The horizontal axis is logarithmic)*

The maximum value of yield strength occurs at 0.167 s^{-1} and the minimum value at 1.67 s^{-1}, which increases and then decreases overall. According to Figure 4.5, the strain at fracture is

positively correlated with the strain rate. No significant correlation was found between Young's modulus and strain rate.

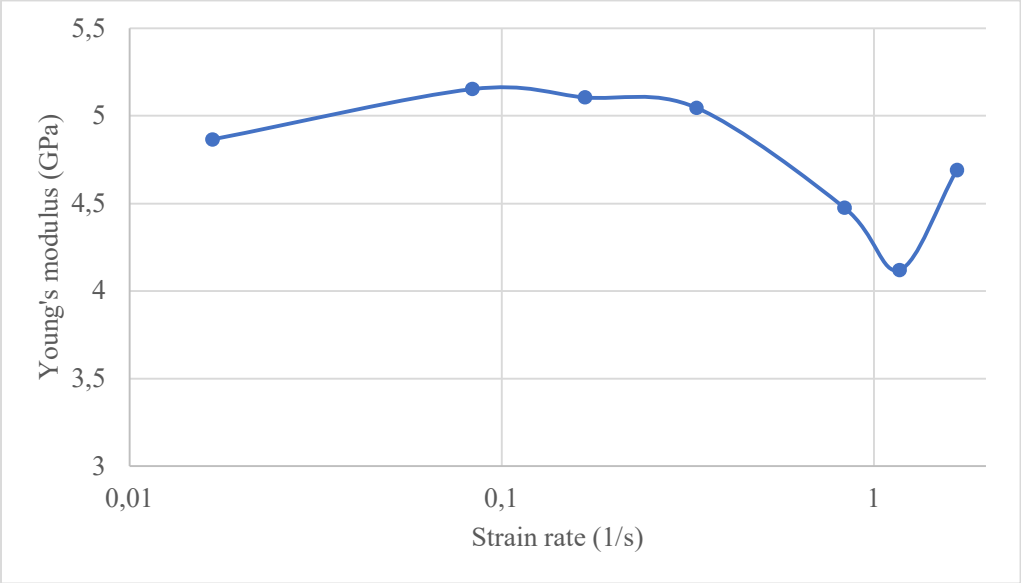

Figure 5.3: *Young's modulus-strain rate graph of TFA (The horizontal axis is logarithmic)*

5.3. Comparison of TFA and TBA behavior at various strain rates

The mechanical properties of Tetra Pak TFA and TBA paperboards at lower strain rates (from 0.0167 s^{-1} to 0.167 s^{-1}) that were obtained in this study are consistent with those reported in other studies in the literature. The two materials show the same trend at strain rates higher than 0.167s^{-1} which are not tested in previous study.

The difference in appearance between these two materials is mainly in the thickness. TBA is made of a combination of multiple layers of paperboard and is approximately four times thicker than TFA. In terms of mechanical properties, the yield strength and Young's modulus of TFA at each strain rate are greater than those of TBA (both cut along MD).

For both materials in all directions, the relationship between stress and strain is initially linear (elastic deformation) and when the stresses both reach a certain value becomes non-linear (plasticity deformation). In addition, the yield strength and strain rate of both materials have a similar variation path (first increase and then decrease), and the strain rates for achieving the maximum yield strength are in the range of 0.133 s^{-1} to 0.167 s^{-1}. This behavior could be explained by viscoplasticity i.e., at the same strain, the higher strain rate the higher stress.

The minimum yield stress always appears at 1.67 s^{-1} and is lower than that at 0.0167 s^{-1}. At higher strain rates, localized damage and weak zones are generated at multiple locations within the material, and the overall ultimate strain of the material grows[13]. This is also reflected in the multiple wrinkles of the samples at higher strain rates, which can be seen more clearly in

CD of the TFA material (Figure 4.12).

There is no considerable difference in strain between the two materials cut along the MD. In MD, the Young's modulus for TBA is approximately double that in TFA.

5.4. Recommendations to Tetra Pak for optimizing existing technology

Based on the experimental results, we can now say that the yield strength of both materials reaches its maximum value at a strain rate of about 0.167 s^{-1}. Therefore, this speed level can be considered the least optimal for mechanical operations on packaging materials. Higher strain rates will not only increase overall productivity but will also lead lower loads on the machine parts during the operation. Furthermore, the probability of paperboard fracture at higher strain rates also seems to be lower, which may improve the stability of packaging process. Therefore, in the actual filling process, this conclusion can be considered together with the packaging speed to determine the optimal working speed of the machine, thus balancing productivity and packaging quality.

In addition, the yield strength of TBA material is not as high as TFA may be related to the thickness of the paperboard. It is possible to make the paperboard layer thinner while ensuring that the function of the packaging material is not affected, thus adapting it to higher speed processing.

Conclusion

Analysis based on literature survey, tensile testing experiments at various strain rates and microscopic observations, allows the following conclusions to be made.

1) The mechanical properties of TFA and TBA paperboards from Tetra Pak obtained in this study at lower strain rates (*from* 0.0167 s^{-1} to 0.167 s^{-1}*)* are consistent with reports from other studies in the literature. They demonstrate moderate increase in yield strength with the increase of strain rate from 0.0167 s^{-1} to 0.167 s^{-1}. However, tensile testing at higher strain rates from 0.167 s^{-1} to 1.67 s^{-1} reveal an opposite trend of yield strength on strain rate. Such a non-monotonic dependence is discovered for the first time in this work.

2) Deformation and fracture mechanisms of paperboards strongly depend on the orientation of fibers in the material. Materials cut along the MD have higher yield stresses and lower yield strains, while materials cut along the CD have the opposite properties. This dependence is persistent across all strain rates investigated in this work.

In the initial phase of this project the basic composition of the packaging material and the role of each layer in practical applications was clarified in the literature research. Especially, paperboard makes a very important contribution to the overall performance of the packaging material. The study of the literature also reveals that the yield stresses of paperboard, aluminum foil and polymer materials are all positively correlated with the strain rate at the low strain rates experimented with by other researchers and yield strain and strain rate are substantially independent. However, data on the mechanical properties of the material at high strain rates are scarce in the literature, and further testing is needed.

In my experiments, the experimental results at the strain rates from 0.0167 s^{-1} to 0.167 s^{-1} were similar to those of others in the literature. For all range of strain rate (from 0.0167 s^{-1} to 1.67 s^{-1}) I tested, the yield strengths of the samples were first increased and then decreased in this strain rate range, and the maximum value was obtained at about 0.167 s^{-1}. The strain was basically positively correlated with the strain rate, and the Young's modulus was not significantly related to it.

The appearance of the samples after stretching is consistent with the experimental data, therefore, the above experimental results can be explained by the arrangement of the fibers in the cardboard and the way in which they fracture. The fibers themselves have a high strength and low elongation, resulting in higher yield stresses but lower strains in the board cut along the MD. The smaller interaction forces between the parallel-aligned fibers lead to the experimental results for CD.

For deformations at lower strain rate ($\leqslant$ 0.167 s^{-1}), the rate of internal crack expansion in the material due to stretching affects its strength and yield stress. For example, at a loading rate of 0.167 s^{-1} the cracks do not have time to expand, resulting in higher strength and yield stresses compared to 0.0167 s^{-1}. This is a similar principle to that of materials such as metals and ceramics. At higher strain rates, however, other changes may have occurred in the fibers in the

board, resulting in a loss of strength and an increase in elongation. This mechanism requires further research.

The differences in appearance and mechanical properties between TBA and TFA were also researched in the experiments. The difference in their material composition caused a four times difference in thickness and a delamination fracture in TBA during stretching. This had an effect on the yield strength and Young's modulus of the paperboard, with TFA being larger in both properties.

Through the above study, data for the mechanical properties of both paperboard materials at various strain rates were obtained, which can help to confirm their adaptability to the folding and sealing speeds of high-speed filling machines, as well as to the high speeds of paper straws when bending. This contributes to the further optimization of the packaging materials and the adaptation of the materials to the subsequent processing.

Future work

Only the macroscopic changes in the two materials have been studied in this paper, and the mechanism that generated the above experimental results can be further determined and analyzed by microscopic images, composition of materials and production processes in the future. In particular, the causes of the mechanical properties of the samples at high speed to be urgently investigated in order to derive the principles of the properties of paperboard materials at high strain rates.

Additionally, integrating the experimental results obtained in this work into the computational models used at Tetra Pak will contribute to a more systematic and integrated study of the two paperboard materials. Mechanical performance testing at higher strain rates can also be modelled through finite element simulation.

In terms of the application of the packaging material, it should also be studied under different temperature and humidity conditions, thus ensuring that the product performs well in different climates around the world. Other materials used in food packaging at Tetra Pak (for instance, polymer, aluminum foil and composite laminates thereof) should also be investigated at equivalent testing conditions.

References

[1] Packaging material for Tetra Pak carton packages. (n.d.). Tetra Pak. Retrieved February 11, 2022, from https://www.tetrapak.com/solutions/packaging/packaging-material/materials

[2] Robertsson, K., Wallin, M., Borgqvist, E., Ristinmaa, M., & Tryding, J. (2021). A rate-dependent continuum model for rapid converting of paperboard. Applied Mathematical Modelling, 99, pp. 497–513.

[3] Nazarinezhad Giashi, A., Gereke, T., Mbarek, T., & Cherif, C. (2021). Novel Dynamic Test Methods for Paperboard Composite Structures. Experimental Techniques.

[4] Bolzon, G., Cornaggia, G., Shahmardani, M., Giampieri, A., & Mameli, A. (2015). Aluminum Laminates in Beverage Packaging: Models and Experiences. Beverages, 1(3), 183–193.

[5] FIELD, J. (2004). Review of experimental techniques for high rate deformation and shock studies. International Journal of IMPact Engineering.

[6] Allaoui, S., Aboura, Z., & Benzeggagh, M. (2009). Phenomena governing uni-axial tensile behaviour of paperboard and corrugated cardboard. Composite Structures, 87(1), 80–92.

[7] Siviour, C. R., & Jordan, J. L. (2016). High Strain Rate Mechanics of Polymers: A Review. Journal of Dynamic Behavior of Materials, 2(1), 15–32.

[8] Malmberg, C., & Käck, B. (2015) Aluminium foil at multiple length scales, mechanical tests and numerical simulations in Abaqus. http://lup.lub.lu.se/student-papers/record/7451137

[9] Packaging materials | Division of Solid Mechanics. (2019, January 15). Packaging Materials. Retrieved March 4, 2022, from https://www.solid.lth.se/research/packaging-materials/

[10] Robertsson, K., Borgqvist, E., Wallin, M., Ristinmaa, M., Tryding, J., Giampieri, A., & Perego, U. (2018). Efficient and accurate simulation of the packaging forming process. Packaging Technology and Science, 31(8), 557-566.

[11] Plc, R. (n.d.). Renishaw: InstronÂ® case study. Renishaw. Retrieved April 30, 2022, from https://www.renishaw.cz/cs/instron-equips-its-new-electropuls-linear-torsion-tester-with-advanced-renishaw-encoders--29004

[12] Tetra Pak® A1 för TFA aseptisk förpackning till låg kostnad. (n.d.). Tetra Pak. Retrieved April 30, 2022, from https://www.tetrapak.com/sv-se/solutions/packaging/filling-machines/tetra-pak-a1-for-tfa

[13] LIAN Xiaogen, LU Lixin, WU Jian, et al. Testing and Characterization of Mechanical Properties and Strain Rate Dependence of Composite Paperboard[J]. Journal of Nanjing University of Aeronautics & Astronautics, 2020,52(3), 438-444.

[14] Shui-sheng, Y., Yu-bin, L., & Yong, C. (2013). The strain-rate effect of engineering materials and its unified model. Latin American Journal of Solids and Structures, 10(4), 833–844.

[15] Tetra Fino Aseptic - a low cost carton pouch. (n.d.). Tetra Pak.

https://www.tetrapak.com/solutions/packaging/packages/tetra-fino-aseptic#:%7E:text=Tetra%20Fino%C2%AE%20Aseptic%20guarantees,value%20in%20a%20friendly%20format!

[16] Tetra Brik Aseptic carton packages for liquid foods. (n.d.). Tetra Pak. https://www.tetrapak.com/solutions/packaging/packages/tetra-brik-aseptic

[17] Tetra Pak® E3 with eBeam technology. (n.d.). Tetra Pak. https://www.tetrapak.com/solutions/packaging/filling-machines/tetra-pak-e3-ebeam

[18] Rullifank, K. F., Roefinal, M. E., Kostanti, M., Sartika, L., & Evelyn. (2020). Pulp and paper industry: An overview on pulping technologies, factors, and challenges. IOP Conference Series: Materials Science and Engineering, 845(1), 012005. https://doi.org/10.1088/1757-899x/845/1/012005

[19] Digital Microscope - VHX-6000 | KEYENCE International Belgium. (n.d.). Digital Microscope. https://www.keyence.eu/products/microscope/digital-microscope/vhx-6000/models/vhx-6000/

[20] Tensile test. (n.d.). Tensile test. https://www.teesim.com/Theory/MAT01/MAT01.html

[21] Wiklund, M., Brismar, H., & Önfelt, B. (2012). Acoustofluidics 18: Microscopy for acoustofluidic micro-devices. Lab on a Chip, 12(18), 3221.

[22] Andreasson, E. (2022, May 2). Personal communication on paperboard used in the TBA-packages [SEM micrographs].

[23] Andreasson, E. (2022, May 2). Personal communication on paperboard used in the TFA-packages [SEM micrographs].

[24] Wikipedia contributors. (2022, July 6). Stress–strain curve. Wikipedia. Retrieved July 11, 2022, from https://en.wikipedia.org/wiki/Stress%E2%80%93strain_curve